

-A133755

RIA-83-U476

TECHNICAL  
LIBRARY

AD A-133 755

TECHNICAL REPORT ARBRL-TR-02525

SOME AERODYNAMIC CHARACTERISTICS OF A  
PROJECTILE SHAPE WITH A NONAXISYMMETRIC  
BOATTAIL AT MACH NUMBERS OF 0.91 AND 3.02

Lyle D. Kayser  
Fred Whiton, Jr.

September 1983



US ARMY ARMAMENT RESEARCH AND DEVELOPMENT COMMAND  
BALLISTIC RESEARCH LABORATORY  
ABERDEEN PROVING GROUND, MARYLAND

Approved for public release; distribution unlimited.

Destroy this report when it is no longer needed.  
Do not return it to the originator.

Additional copies of this report may be obtained  
from the National Technical Information Service,  
U. S. Department of Commerce, Springfield, Virginia  
22161.

The findings in this report are not to be construed as  
an official Department of the Army position, unless  
so designated by other authorized documents.

*The use of trade names or manufacturers' names in this report  
does not constitute endorsement of any commercial product.*

UNCLASSIFIED

SECURITY CLASSIFICATION OF THIS PAGE (When Data Entered)

REPORT DOCUMENTATION PAGE		READ INSTRUCTIONS BEFORE COMPLETING FORM
1. REPORT NUMBER TECHNICAL REPORT ARBRL-TR-02525	2. GOVT ACCESSION NO.	3. RECIPIENT'S CATALOG NUMBER
4. TITLE (and Subtitle)  SOME AERODYNAMIC CHARACTERISTICS OF A PROJECTILE SHAPE WITH A NONAXISYMMETRIC BOATTAIL AT MACH NUMBERS OF 0.91 AND 3.02		5. TYPE OF REPORT & PERIOD COVERED  Final
7. AUTHOR(s)  L. D. Kayser and F. Whiton, Jr.		6. PERFORMING ORG. REPORT NUMBER
9. PERFORMING ORGANIZATION NAME AND ADDRESS  U.S. Army Ballistic Research Laboratory ATTN: DRDAR-BLL Aberdeen Proving Ground, Maryland 21005		10. PROGRAM ELEMENT, PROJECT, TASK AREA & WORK UNIT NUMBERS  RDT&E 1L162618AH80
11. CONTROLLING OFFICE NAME AND ADDRESS  US Army Armament Research & Development Command US Army Ballistic Research Laboratory (DRDAR-BLA-S) Aberdeen Proving Ground, MD 21005		12. REPORT DATE  September 1983
14. MONITORING AGENCY NAME & ADDRESS (if different from Controlling Office)		13. NUMBER OF PAGES  48
		15. SECURITY CLASS. (of this report)  Unclassified
		15a. DECLASSIFICATION/DOWNGRADING SCHEDULE
16. DISTRIBUTION STATEMENT (of this Report)  Approved for public release; distribution unlimited.		
17. DISTRIBUTION STATEMENT (of the abstract entered in Block 20, if different from Report)		
18. SUPPLEMENTARY NOTES		
19. KEY WORDS (Continue on reverse side if necessary and identify by block number)  Projectile Stability Nonaxisymmetric Nonconical Boattails Experimental Data Computations		
20. ABSTRACT (Continue on reverse side if necessary and identify by block number)  Some aerodynamic properties of a projectile shape with a nonaxisymmetric boattail are presented. The boattail is formed by machining three flat surfaces which are equally spaced and inclined seven degrees to the model axis. Aerodynamic forces obtained by strain-gage balance measurements are presented for angles of attack up to 15° and for various roll orientations of the model. Because the effect of roll orientation on coefficient data is quite small, coefficients are presented in incremental form so that the effect of roll can be graphically amplified. A limited quantity of the data is compared to		

UNCLASSIFIED

SECURITY CLASSIFICATION OF THIS PAGE(When Data Entered)

20. ABSTRACT (Continued)

computational results for Mach 3.02. The results of this study support previous studies which show that nonaxisymmetric boattail shapes can improve the static stability of projectiles.

UNCLASSIFIED

SECURITY CLASSIFICATION OF THIS PAGE(When Data Entered)

## TABLE OF CONTENTS

	<u>Page</u>
LIST OF ILLUSTRATIONS.....	5
I INTRODUCTION.....	7
II EXPERIMENTS.....	8
III DATA PROCESSING.....	9
IV ERROR ANALYSIS.....	9
V COMPUTATIONS.....	10
VI RESULTS.....	10
VII CONCLUSIONS.....	12
REFERENCES.....	38
APPENDIX A - TABULATED DATA.....	39
LIST OF SYMBOLS.....	45
DISTRIBUTION LIST.....	47

## LIST OF ILLUSTRATIONS

<u>Figure</u>		<u>Page</u>
1	Model Geometry, SOCBT Axisymmetric Shape.....	13
2	Nonconical Boattail Geometry.....	14
3	Model Roll Orientation.....	15
4	Cubic Spline Curve Fit, $M_\infty = 0.91$ , $\phi = 20^\circ$ .....	16
5	Uncorrected Incremental Coefficient Data, SOCBT-NC.....	17
	a. $\Delta C_N$ vs $\phi$ , $M_\infty = 0.91$ .....	17
	b. $\Delta C_N$ vs $\phi$ , $M_\infty = 3.02$ .....	18
	c. $\Delta C_Y$ vs $\phi$ , $M_\infty = 3.02$ .....	19
6	Comparison of Computation and Experiment, SOCBT-NC, $\phi = 0^\circ$ .....	20
	a. $C_N$ vs $\alpha$ .....	20
	b. $C_m$ vs $\alpha$ .....	21
7	Comparison of Nonconical and Axisymmetric Shapes.....	22
	a. $C_{N\alpha}$ and $C_{m\alpha}$ vs $\phi$ , $M_\infty = 0.91$ .....	22
	b. $C_{N\alpha}$ and $C_{m\alpha}$ vs $\phi$ , $M_\infty = 3.02$ .....	23
8	Computational Results, SOCBT-NC, $M_\infty = 3.02$ .....	24
	a. $C_N$ vs $Z/D$ , $\alpha = 6^\circ$ .....	24
	b. $C_Y$ vs $Z/D$ , $\alpha = 10^\circ$ .....	25
9	Incremental Coefficient Values, SOCBT-NC.....	26
	a. $\Delta C_N$ vs $\phi$ , $M_\infty = 0.91$ .....	26
	b. $\Delta C_m$ vs $\phi$ , $M_\infty = 0.91$ .....	27
	c. $\Delta C_Y$ vs $\phi$ , $M_\infty = 0.91$ .....	28
	d. $\Delta C_n$ vs $\phi$ , $M_\infty = 0.91$ .....	29
	e. $\Delta C_\ell$ vs $\phi$ , $M_\infty = 0.91$ .....	30
10	Incremental Coefficient Values, SOCBT-NC.....	31
	a. $\Delta C_N$ vs $\phi$ , $M_\infty = 3.02$ .....	31
	b. $\Delta C_m$ vs $\phi$ , $M_\infty = 3.02$ .....	32
	c. $\Delta C_Y$ vs $\phi$ , $M_\infty = 3.02$ .....	33

LIST OF ILLUSTRATIONS (Cont'd)

<u>Figure</u>		<u>Page</u>
d.	$\Delta C_n$ vs $\phi$ , $M_\infty = 3.02$ .....	34
e.	$\Delta C_\lambda$ vs $\phi$ , $M_\infty = 3.02$ .....	35
11	Incremental Normal Force Coefficients, Computation and Experiment, $M_\infty = 3.02$ .....	36

## I. INTRODUCTION

The objective of the wind tunnel test program was to obtain data on a nonaxisymmetric projectile shape which could be used for comparison with computation. Most of the computational effort within the Aerodynamics Research Branch of the Launch and Flight Division has been directed toward axisymmetric projectile shapes; however, recent efforts have been in the direction of increasing the computational capability for nonaxisymmetric shapes, including finned bodies. The specific projectile shape with a nonaxisymmetric boattail, as shown in Figures 1 and 2, was chosen for the experiment as a result of our past experience with this nonconical projectile shape. The aerodynamic characteristics of nonaxisymmetric boattail shapes have been examined to some degree at the BRL since 1974. The terms nonaxisymmetric, nonconical, and unconventional are used interchangeably in this report. The nonaxisymmetric boattail is usually formed by a number of flat surfaces inclined to the model axis as opposed to the conventional axisymmetric conical boattail. For example, three surfaces of sufficient length would develop into a triangular base (Figure 2), or four flat surfaces would develop into a square base. All data for this report are for the one-caliber seven-degree triangular boattail shown in Figure 2. Platou<sup>1-4</sup> has examined several nonconical boattail configurations in recent years including triangular, square, cruciform, and modified square and triangular boattails with added lifting surfaces. The general findings of Platou are that nonconical boattails reduce drag and increase the static stability of projectiles when compared to conical boattails. For spinning projectiles, the boattail surfaces must be twisted at the same rate as the rifling twist to avoid an excessive despinning moment. Zumwalt's<sup>5</sup> trough-like base region has similarities to the cruciform configuration of Platou. Zumwalt found that the effect of adding the trough to the base was to increase the base pressure by a factor of two at Mach 2

- 
1. Platou, A.S., "An Improved Projectile Boattail," ARBRL-MR-2395, U.S. Army Ballistic Research Laboratory, ARRADCOM, Aberdeen Proving Ground, Maryland 21005, July 1974 (AD 785520).
  2. Platou, A.S., and Nielson, G.I.T., "An Improved Projectile Boattail. Part II," BRL R 1866, U.S. Army Ballistic Research Laboratory, ARRADCOM, Aberdeen Proving Ground, Maryland 21005, March 1976 (AD A024073).
  3. Platou, A.S., "An Improved Projectile Boattail. Part III," ARBRL-MR-2644, U.S. Army Ballistic Research Laboratory, ARRADCOM, Aberdeen Proving Ground, Maryland 21005, July 1976 (AD B012781L).
  4. Platou, A.S., "An Improved Projectile Boattail. Part IV," ARBRL-MR-02826, U.S. Army Ballistic Research Laboratory, ARRADCOM, Aberdeen Proving Ground, Maryland 21005, April 1978 (AD B027520L).
  5. Zumwalt, G.W., "Experiments on Three-Dimensional Separating-and-Reattaching Flows," AIAA Paper No. 81-0259, AIAA 19th Aerospace Sciences Meeting, January 1981.

and a factor of four at Mach 3. Reference 6 compares measured pressures on a nonconical boattail with pressures obtained by inviscid computation. Qualitatively, the inviscid computation predicted the correct trends; however, the quantitative agreement was generally poor. More recent computations by Sturek<sup>7</sup> using a parabolized Navier-Stokes code showed a much improved agreement in comparison of pressure distributions over the nonconical boattail. Reference 6 also reports comparisons of experimental nonconical static stability results with computational results for axisymmetric shapes having similar moments of inertia characteristics. The results show that the nonconical boattail increases the static stability and in some cases the stability is greater than that of a straight cylindrical ( $0^\circ$ ) boattail. Danberg and Tschirschnitz<sup>8</sup> obtained pressure measurements in the boattail region of axisymmetric and nonaxisymmetric configurations at transonic speeds. Integration of pressures over the boattails showed that the nonaxisymmetric (triangular) boattail reduced total projectile drag by approximately 15% and increased the static stability with respect to the conical boattail configuration. The static stability for the nonconical shape was, however, not as good as the high drag straight cylindrical configuration. Platou<sup>9</sup> has extended the concept of the nonconical boattail to forward facing flats on the model, which gives the model corkscrew-like characteristics. Reference 9 describes a study of corkscrew configurations which have the potential of further decreasing projectile drag.

## II. EXPERIMENTS

The wind tunnel tests were conducted in the Supersonic Wind Tunnel No. 2 of the Naval Surface Weapons Center (NSWC), White Oak Laboratory, at Mach Numbers of 0.91 and 3.02. Data were acquired at angles of attack of -5 to 15 degrees for  $M = 0.91$ , and -5 to  $12.5^\circ$  for  $M = 3.02$ . The procedure of acquiring the data was to fix the roll orientation to one of the positions shown in

- 
6. Kayser, L.D., and Sturek, W.B., "Aerodynamic Performance of Projectiles with Axisymmetric and Non-Axisymmetric Boattails," ARBRL-MR-03022, U.S. Army Ballistic Research Laboratory, ARRADCOM, Maryland 21005, May 1980 (AD A086091).
  7. Schiff, L.B., and Sturek, W.B., "Numerical Simulation of Steady Supersonic Flow Over an Ogive Cylinder Boattail Body," ARBRL-TR-02363, U.S. Army Ballistic Research Laboratory, ARRADCOM, Aberdeen Proving Ground, Maryland 21005, September 1981 (AD A106060).
  8. Danberg, J.E., and Tschirschnitz, R.H., "Transonic Pressure Distribution and Boundary Layer Characteristic of a Projectile with an Asymmetric Afterbody," Technical Report 243, University of Delaware, June 1981.
  9. Platou, A.S., "Decreasing the Flight Time of Bullets by Improving Its Aerodynamic Characteristics," ARBRL-MR-03103, U.S. Army Ballistic Research Laboratory, ARRADCOM, Aberdeen Proving Ground, Maryland 21005, May 1981 (AD B058203L).

Figure 4, and then pitch the model through the angle-of-attack range. Aerodynamic force and moment measurements were obtained by means of an internal strain-gage balance. The following forces and moments were measured: normal force, pitching moment, side force, yawing moment, and rolling moment. Supply pressure and temperature for the  $M = 3.02$  runs were 221 kPa (32 psia) and  $322^\circ K$ , respectively, which yielded a model-length Reynolds number of  $5.0 \times 10^6$ . The supply pressure and temperature for the  $M = 0.91$  runs were 101 kPa (14.7 psia) and  $322^\circ K$ , which gave a model-length Reynolds Number of  $4.5 \times 10^6$ .

### III. DATA PROCESSING

Data were supplied by the NSWC with the usual bias corrections for flow angularity; for example, it is assumed that normal force and pitching moments must be zero at zero angle of attack for appropriate configurations. An initial examination of the data showed that the effects of varying the roll attitude of the model were very small; for this reason, the data were further processed with the hope that the effects of roll could be adequately extracted. The pitch plane data, for a given roll orientation, was fitted with a cubic spline; Figure 4 is an example of such a curve fit. When all data had been curve fitted, incremental coefficient values were computed by subtracting coefficient values at zero roll angle from coefficient values at positive angles of roll. Figures 5a, b, c are examples of some results. Some of the results are reasonably good (Figure 5a) and other results are rather poor (Figures 5b and c). Conditions of symmetry dictate, theoretically, that  $C_N$  and  $C_m$  are symmetrical about  $\phi = 60^\circ$  and that  $C_y$ ,  $C_n$ , and  $C_\ell$  have odd symmetry about  $\phi = 60^\circ$ . Therefore, in an attempt to further improve the quality of results, conditions of symmetry were forced upon the data by appropriate averaging.

### IV. ERROR ANALYSIS

Initially, it was considered that the order of magnitude of the error could be estimated by assuming a measurement accuracy of one percent of the full-scale measuring capacity. Table 1 shows this error in percent of the maximum coefficient value measured. For normal force and pitching moment coefficients, the 1% criterion would indicate good quality data. The 1% criterion for incremental coefficient values at Mach 3.02 gives large errors which are in the range of 94 to 500%, but at Mach 0.91, the 1% criterion is not so severe although it still suggests moderate to large errors of 9 to 52%. It may be difficult to show by conventional error analysis that measurement errors are substantially less than one percent; however, experience has sometimes shown that when bias errors are removed from the data, considerable improvements are exhibited.

Because of symmetry, as indicated above, many comparisons of data repeatability could be made. If it is "assumed" that the correct data value is the average of all repeated measurements, then an indication of the error is the difference between the average value and the measured value. For each coefficient, approximately 10 errors were computed for the angle-of-attack range and a standard deviation computed for each coefficient. These values are tabula-

ted in Table 1 and are believed to be reasonably good indication of error magnitude. The normal force and pitching moment errors vary from 0.1 to 0.3%, which is considered very good. The incremental coefficient values, due to change in roll orientation, vary from good to poor in quality. The standard deviations for Mach 3.02 are seen to be much smaller than the error determined by the one-percent criterion, which indicates that the balance and measuring systems were functioning well. It is surprising to note that the standard deviations for side force and yawing moment at Mach 0.91 are larger than 1% errors. This situation may indicate that some unexplained flow phenomena have existed at the transonic Mach number.

## V. COMPUTATIONS

Recently, Sturek<sup>7</sup> has been using the thin-layer parabolized Navier-Stokes (PNS) code to compute flow over various projectile shapes. The PNS code used is that reported by Schiff and Steger. (Details of the notation, the PNS assumption, derivation of the algorithm, the associated stability analysis, and application of the boundary conditions may be found in Reference 10.) PNS computations were carried out for the nonconical shape at Mach 3 and angles of attack of 4, 6, and 10°. For each angle of attack, a solution was obtained over the axisymmetric portion of the projectile shape; then the solution was picked up and marched over the nonaxisymmetric boattail for boattail orientations of 0 to 60° (see Figure 3) in 10° increments. Generally, 36 circumferential points are used for axisymmetric shapes; however, for this computation the number of points was increased to 72. At each of the 72 points, in the circumferential direction, were 50 points normal to the surface. Thus, at each computational plane normal to the axis of the model there were 3600 points. It should be noted that the spacing of the points was not constant in the normal direction, but the spacing in the circumferential direction was constant at 5° intervals. The total number of computational planes over the entire model was approximately 700 with 120 (of the 700) being placed over the boattail section of the model. The spacing of the points along the longitudinal direction was constant.

## VI. RESULTS

Tabulated results of the experimental data are presented in Appendix A. The tables include normal force and pitching moment coefficient data and incremental coefficient data for normal force, pitching moment, side force, yawing moment, and rolling moment. The incremental coefficient values are referenced to the  $\phi = 0^\circ$  roll orientation; therefore, for side force, yawing moment, and rolling moment, there is no difference between the actual coefficient values and the incremental values.

---

10. Schiff, L.B., and Steger, J.L., "Numerical Simulation of Steady Supersonic Flow," AIAA Journal, Vol. 18, No. 12, December 1980, pp. 1421-1430.

Normal force and pitching moment data at zero roll are presented in Figures 6a and 6b. Mach 3 computations at 4, 6, and 10 degrees angle of attack are included and the agreement between computation and experiment is very encouraging. Similar plots at other roll positions are not included because the effect of roll, as will be shown, is very small. Figures 7a and 7b provide a summary of the static force and moment data for the nonconical boattail (SOCBT-NC) configuration along with data for two axisymmetric configurations -- an ogive cylinder (SOC) and an ogive cylinder with a 7° conical boattail (SOCBT). Coefficients for the axisymmetric SOC and SOCBT shapes are independent of roll orientation and are therefore shown as constant values in Figure 7. At Mach 0.91, we see that the static moment for the nonconical shape does not vary significantly with roll orientation. Also, it is seen that the static moment for the nonconical shape is smaller (more stable) than that of the SOCBT shape, but it is still larger than that of the high drag SOC. Danberg<sup>8</sup> made similar comparisons at Mach 0.94 for the following three afterbody shapes: (1) 1.44 caliber, 7° triangular boattail; (2) 1.44 caliber straight cylindrical boattail; (3) 1.46 caliber axisymmetric boattail (0.96 caliber cylinder + 0.5 caliber, 7° conical). Their findings are similar to the above results and show that even in the most unfavorable orientation, the triangular afterbody is more stable than the conventional conical boattail shape but not as stable as the high drag cylinder. Although no drag results were obtained in this investigation, Danberg found the boattail drag of the triangular shape to be only 48% of the drag of the conventional boattail, which resulted in an estimated overall drag reduction of 15.5%. At Mach 3, Figure 7b, computational results are compared to experiment; the agreement with  $C_{N\alpha}$  is very good but the agreement with  $C_{M\alpha}$  is not quite as good. Both computation and experiment show only slight variations with roll orientation. Again, the nonconical boattail is seen to decrease the static moment with respect to the conical boattail, and at this Mach number (3.0) the static moment is approximately equal to that of the cylindrical boattail shape (SOC).

The small variation of normal force with roll is illustrated, computationally, in Figure 8a where normal force coefficient is plotted on a highly expanded scale and data for all roll positions fall within a rather narrow band. The normal force is seen to increase with distance along the boattail which, acting on the aft end of the model, provides a restoring moment or increased stability; this trend is opposite of that typically observed on conical boattails. The longitudinal variation in side force is shown in Figure 8b. The side force is seen to increase to a maximum at Z/D values of approximately 5.6; then the side force decreases over the remainder of the boattail. This unexpected behavior also occurred at 4° and 6° angles of attack. The final values of side force are seen to be very small and the variation with roll is nearly an order of magnitude smaller than normal force variations. These small values of side force coefficient make it impossible to get a reasonable comparison with experiment.

Incremental coefficient values for the five components of measurement are presented in Figures 9 and 10. Coefficient values at -5° angle of attack would not be expected to equal values at +5° angle of attack. Conditions of symmetry permitted adjustment to the -5° data so that, theoretically, it should equal the +5° data. The difference between the -5° and +5° data is, therefore, an indication of the data quality. The Mach 0.91 normal force and

pitching moment data of Figure 9a and b show a good consistency with angle of attack and are believed to be good quality data. The side force, yawing moment, and rolling moment show a fair degree of consistency and should indicate, qualitatively, the variation of coefficient values with roll. The incremental coefficient values at Mach 3.02, Figures 10 a-e, do not show as good a consistency as the Mach 0.91 data but, nevertheless, the data appear to be of sufficient quality for making qualitative comparisons to computational data. Incremental values of normal force coefficient for computation and experiment are compared in Figure 11. The magnitude and trends of the data compare reasonably well although there is some difference in the overall shape of the curves. The agreement is considered to be fairly good considering the accuracy of the experimental data and the small values being compared.

## VII. CONCLUSIONS

1. The ogive-cylinder model with a 7° nonconical boattail exhibits a smaller static moment (greater static stability) both transonically and supersonically than a similar body with a conventional conical boattail.
2. The variation of  $C_{N\alpha}$  and  $C_{m\alpha}$  are nearly independent of roll orientation for the nonconical shape (SOCBT-NC).
3. The accuracy of the coefficient data are not as good as desired but the data are of sufficient quality to help evaluate computational codes for nonaxisymmetric bodies.

# SOCBT

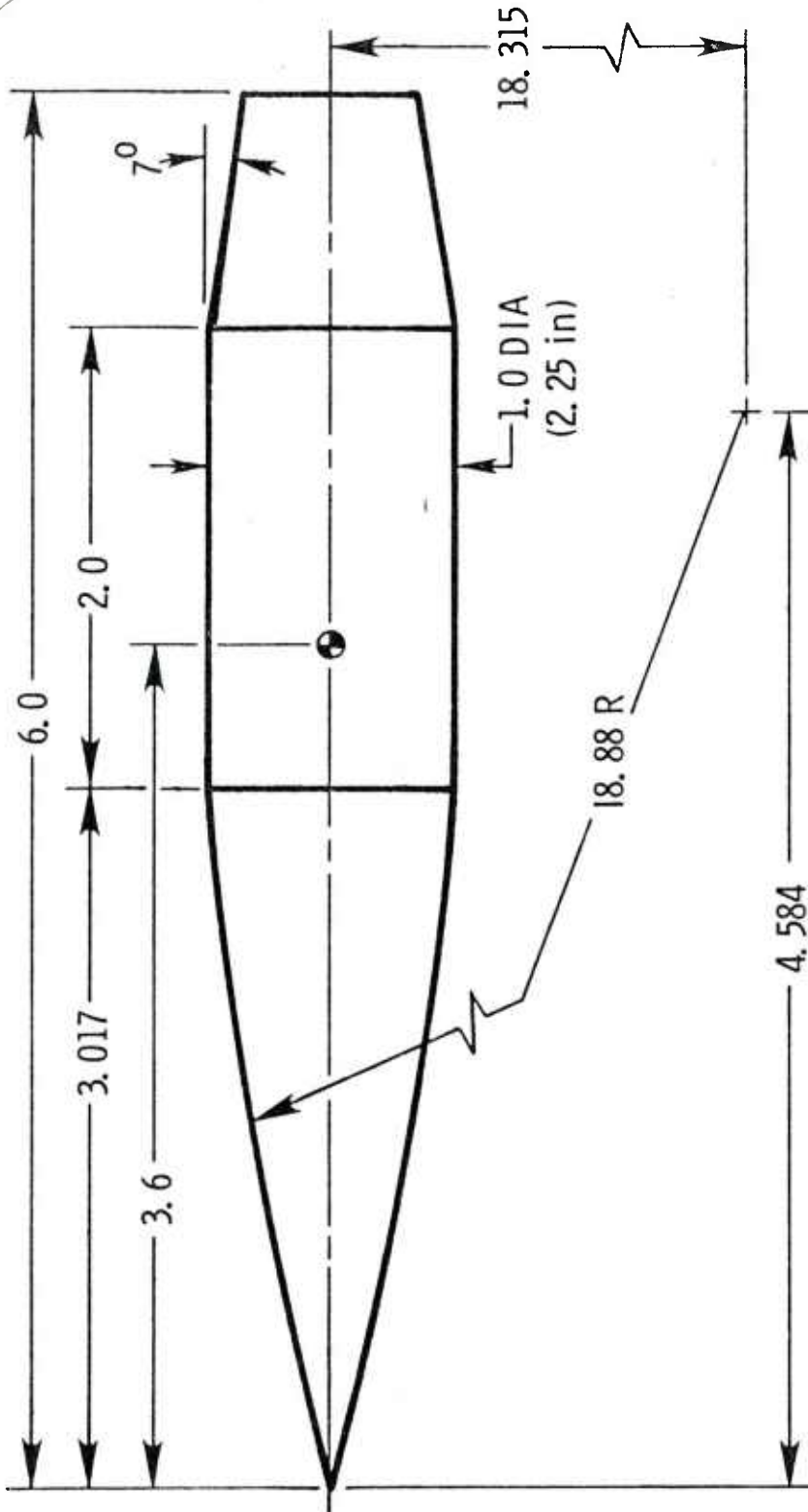


Figure 1. Model Geometry, SOCBT Axisymmetric Shape

# SOCBT-NC

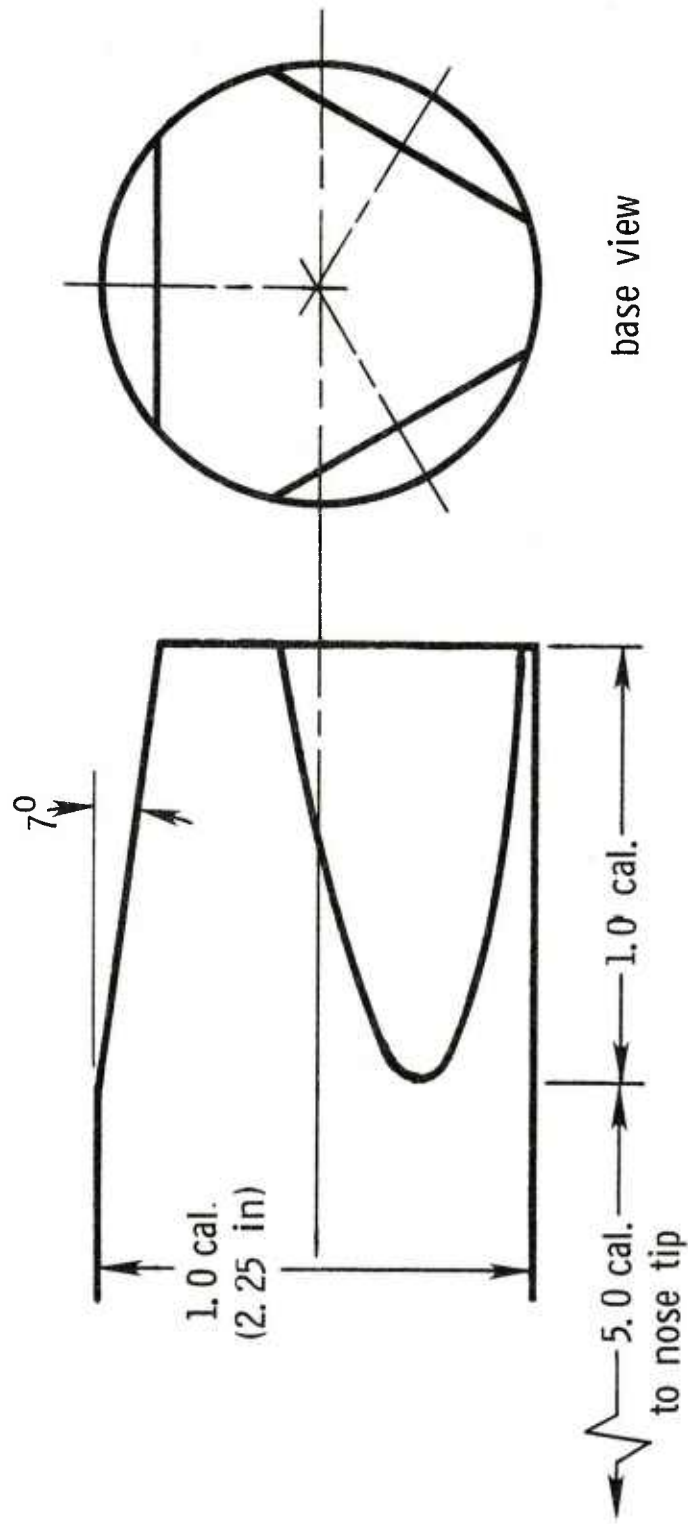


Figure 2. Nonconical Boattail Geometry

## BASE VIEW

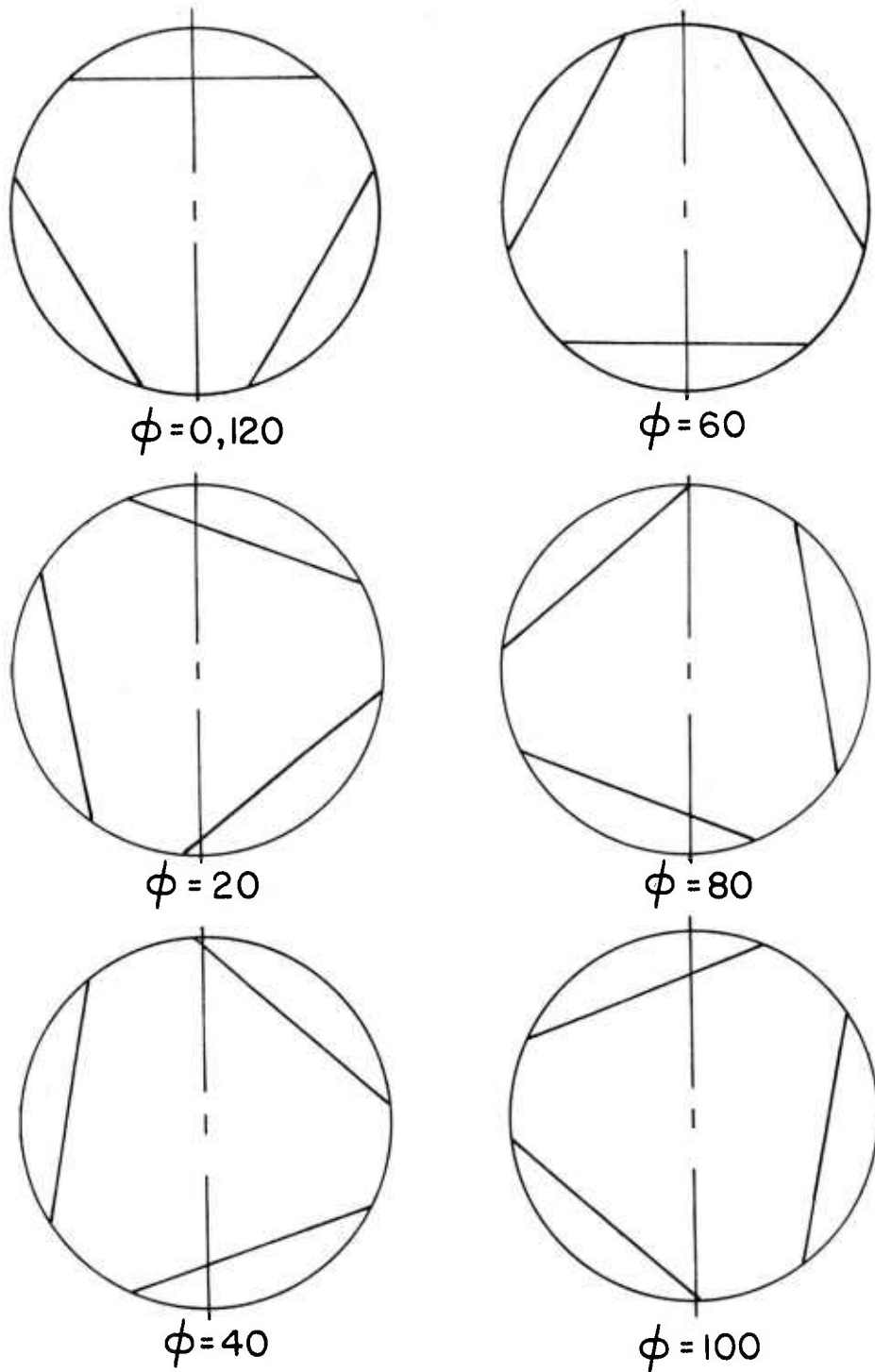


Figure 3. Model Roll Orientation

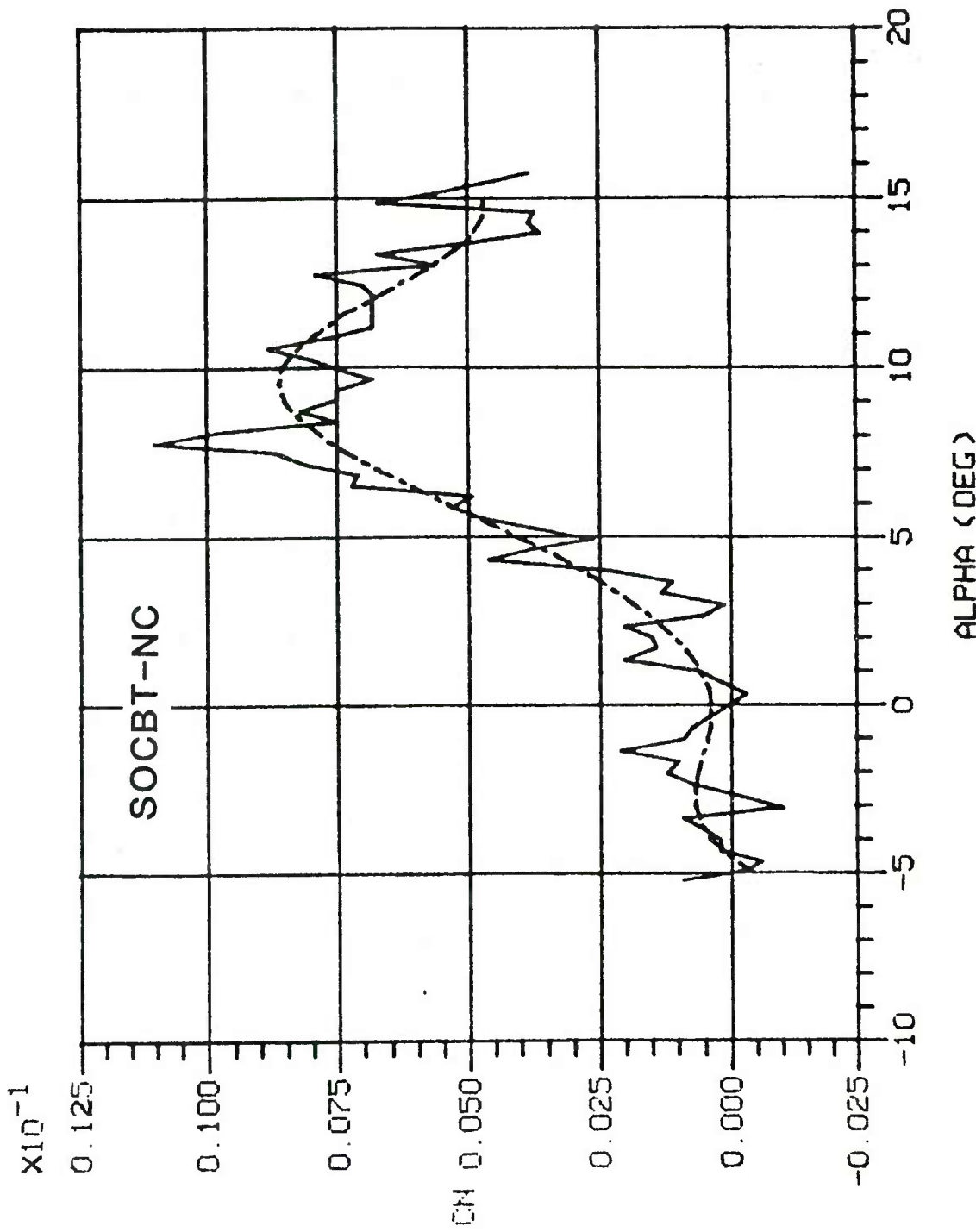


Figure 4. Cubic Spline Curve Fit,  $M_\infty = 0.91$ ,  $\phi = 20^\circ$

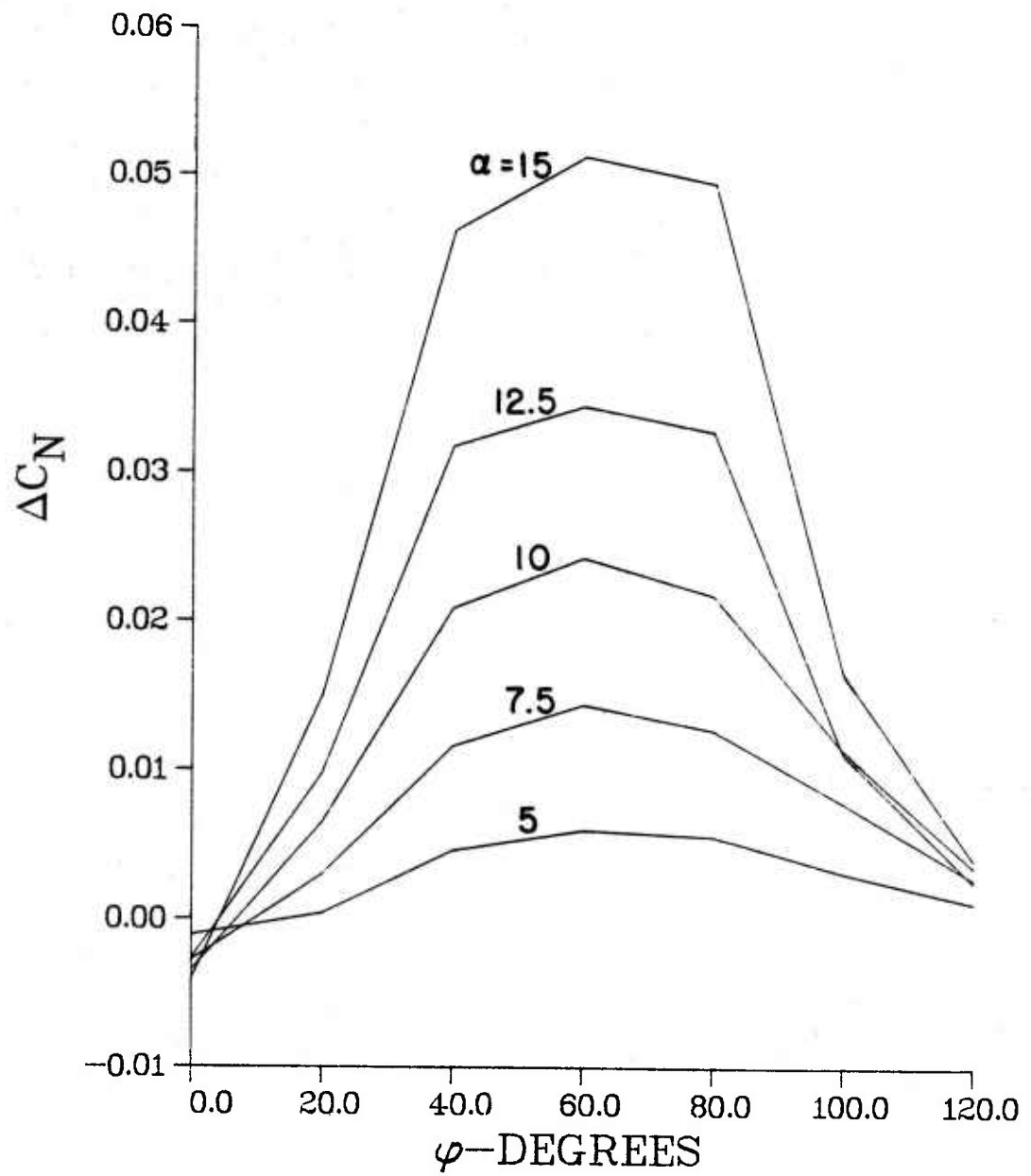


Figure 5. Uncorrected Incremental Coefficient Data, SOCBT-NC

a.  $\Delta C_N$  vs  $\phi$ ,  $M_\infty = 0.91$

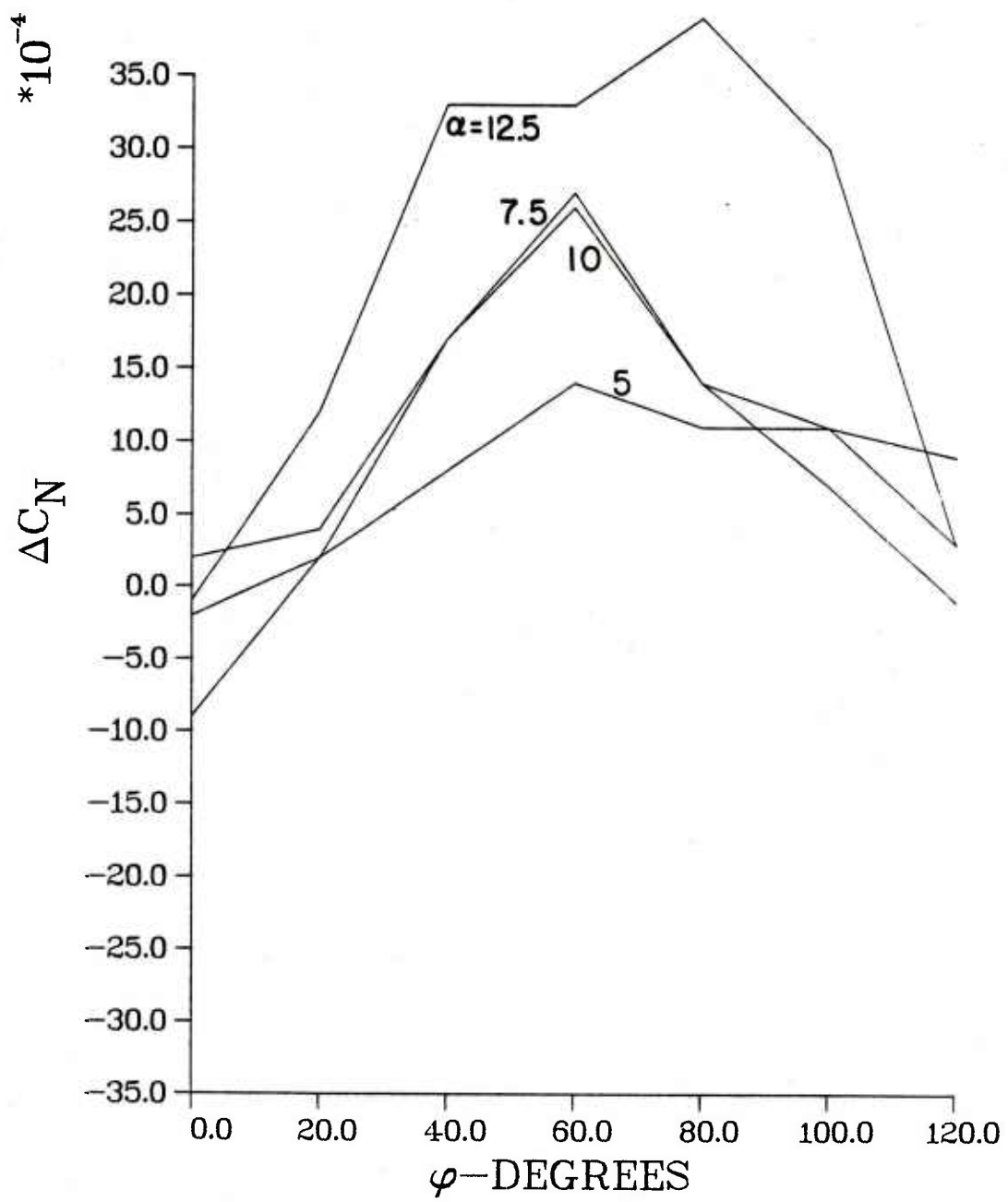


Figure 5. Continued

b.  $\Delta C_N$  vs  $\phi$ ,  $M_\infty = 3.02$

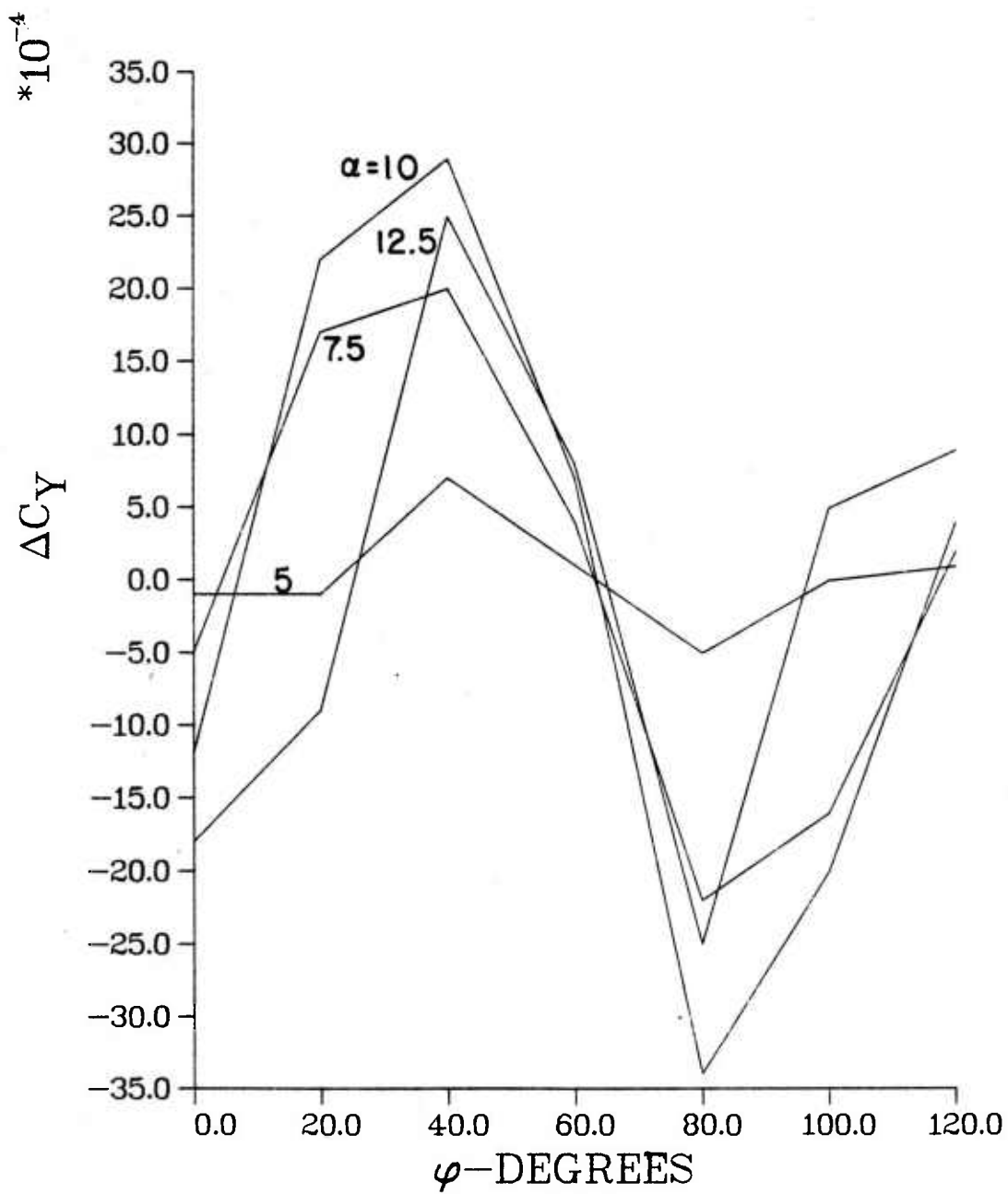


Figure 5. Continued

c.  $\Delta C_Y$  vs  $\phi$ ,  $M_\infty = 3.02$

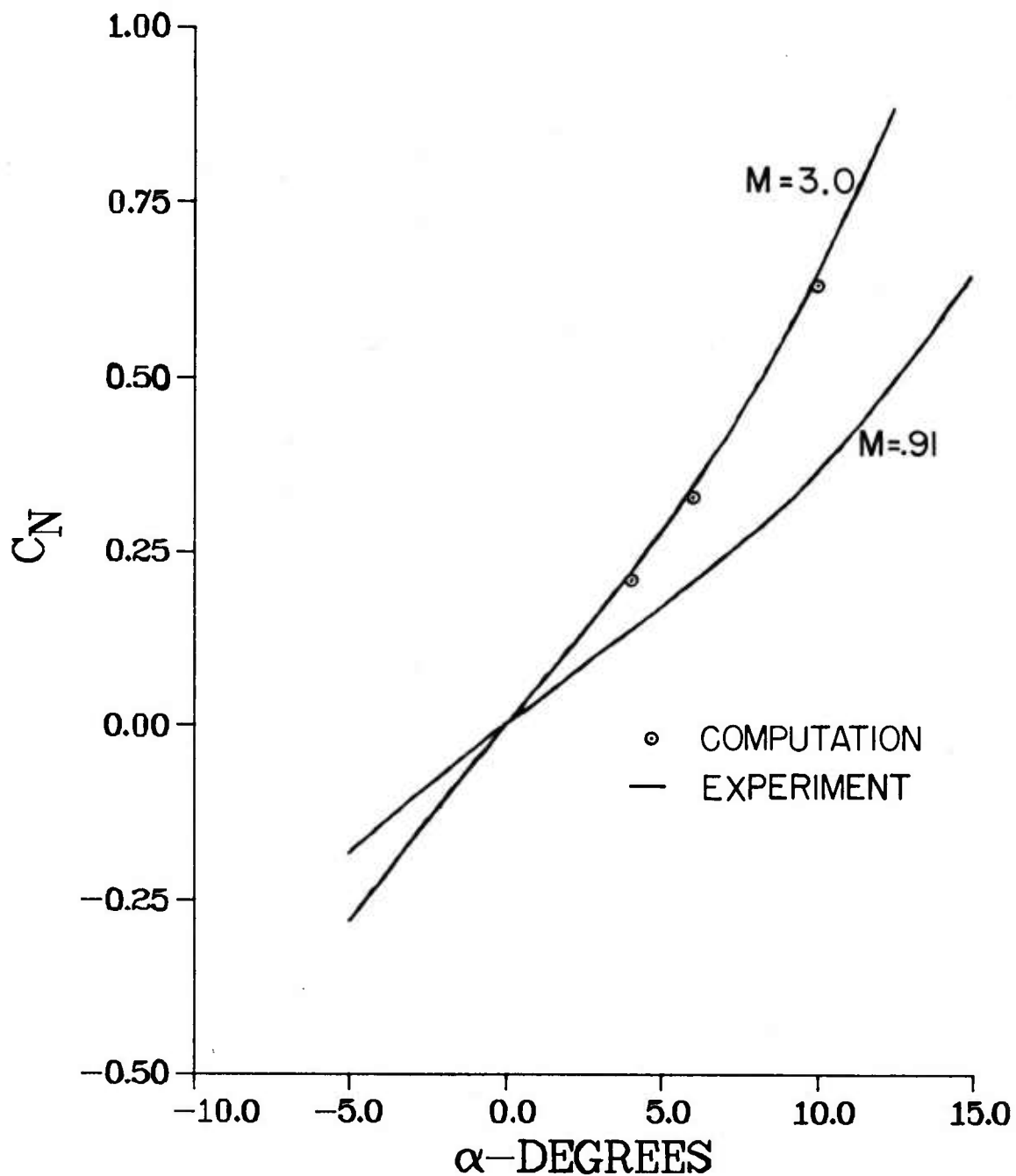


Figure 6. Comparison of Computation and Experiment, SOCBT-NC,  $\phi = 0^\circ$

a.  $C_N$  vs  $\alpha$

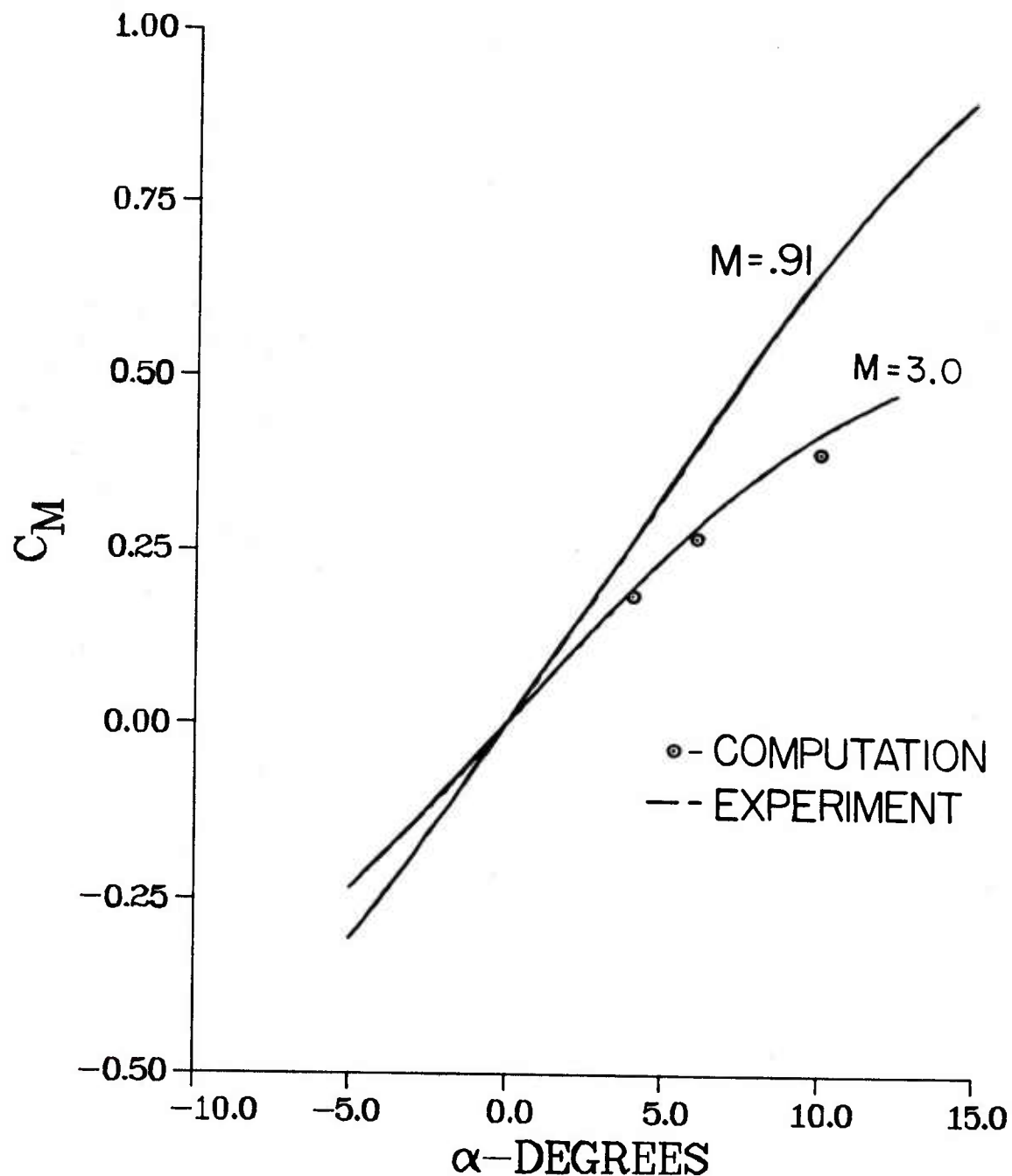


Figure 6. Continued

b.  $C_M$  vs  $\alpha$

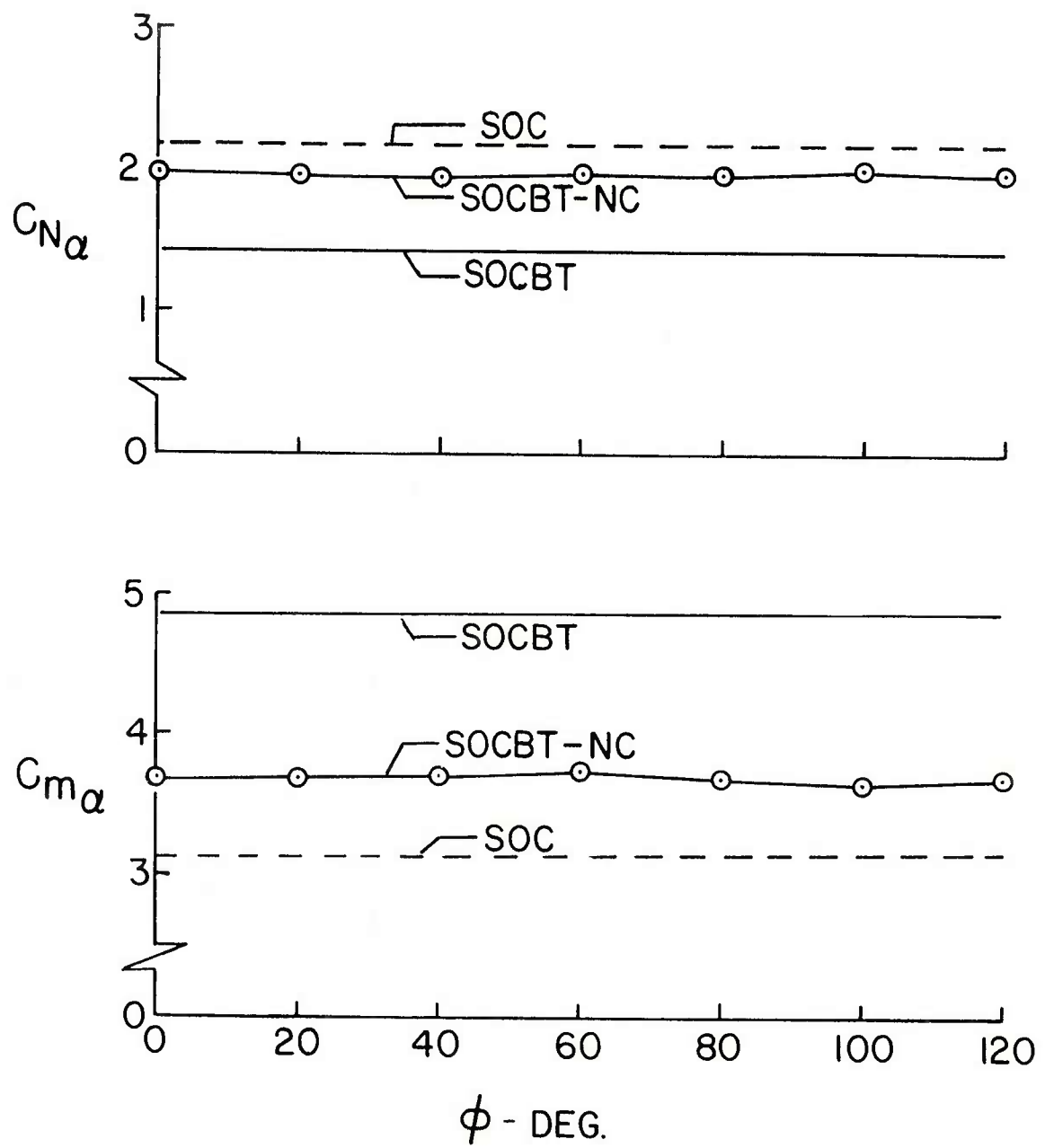


Figure 7. Comparison of Nonconical and Axisymmetric Shapes

a.  $C_{N\alpha}$  and  $C_{m\alpha}$  vs  $\phi$ ,  $M_\infty = 0.91$

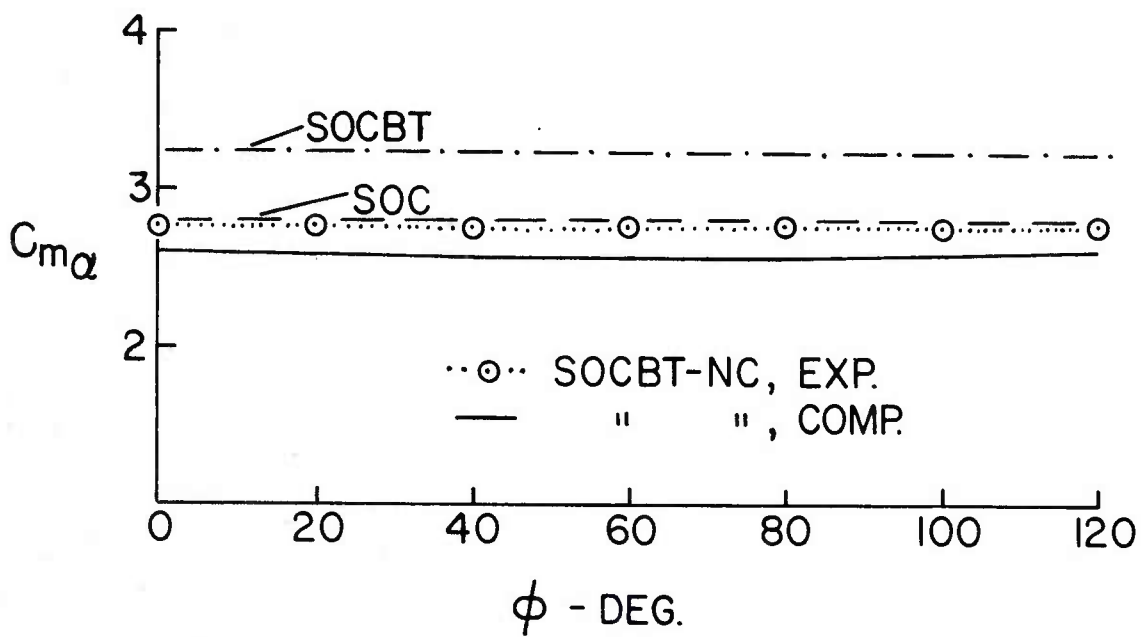
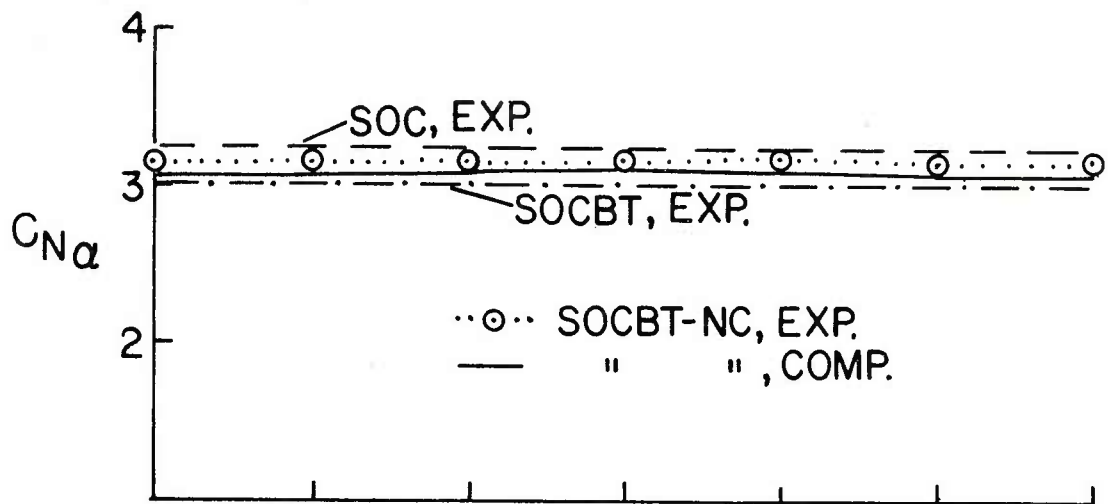


Figure 7. Continued

b.  $C_{N\alpha}$  and  $C_{m\alpha}$  vs  $\phi$ ,  $M_\infty = 3.02$

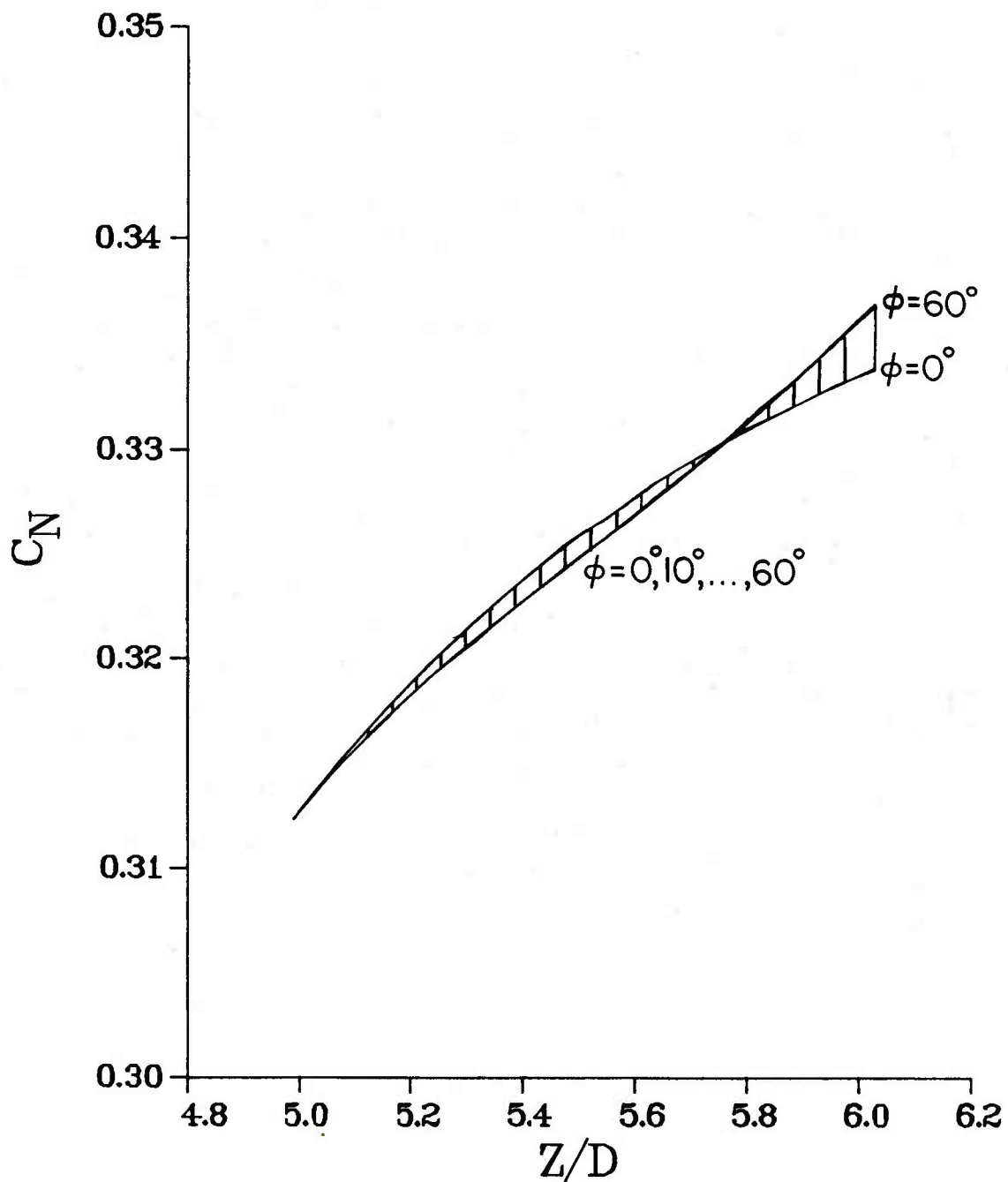


Figure 8. Computational Results, SOCBT-NC,  $M_\infty = 3.02$

a.  $C_N$  vs  $Z/D$ ,  $\alpha = 6^\circ$

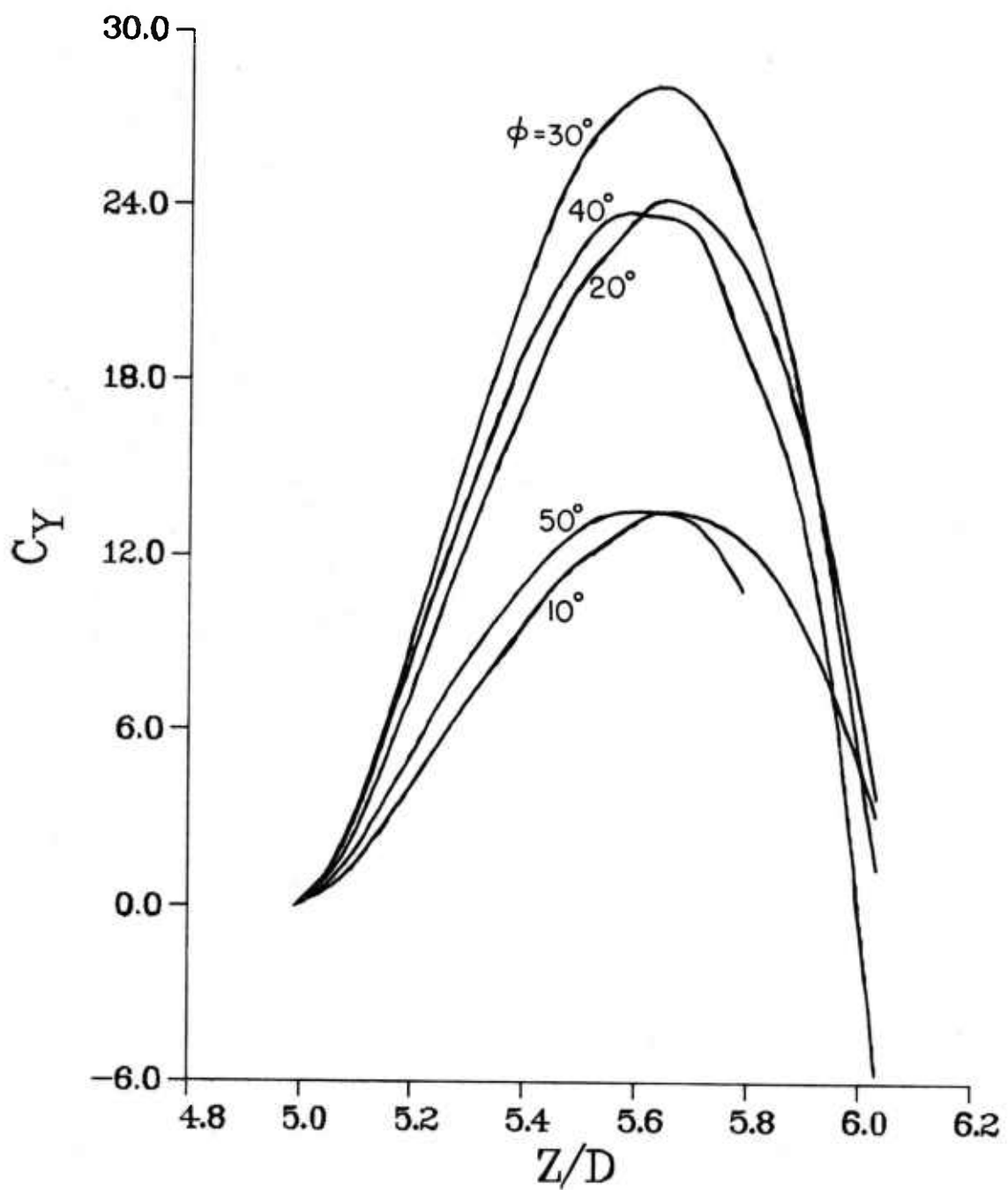


Figure 3. Continued

b.  $C_Y$  vs  $Z/D$ ,  $\alpha = 10^\circ$

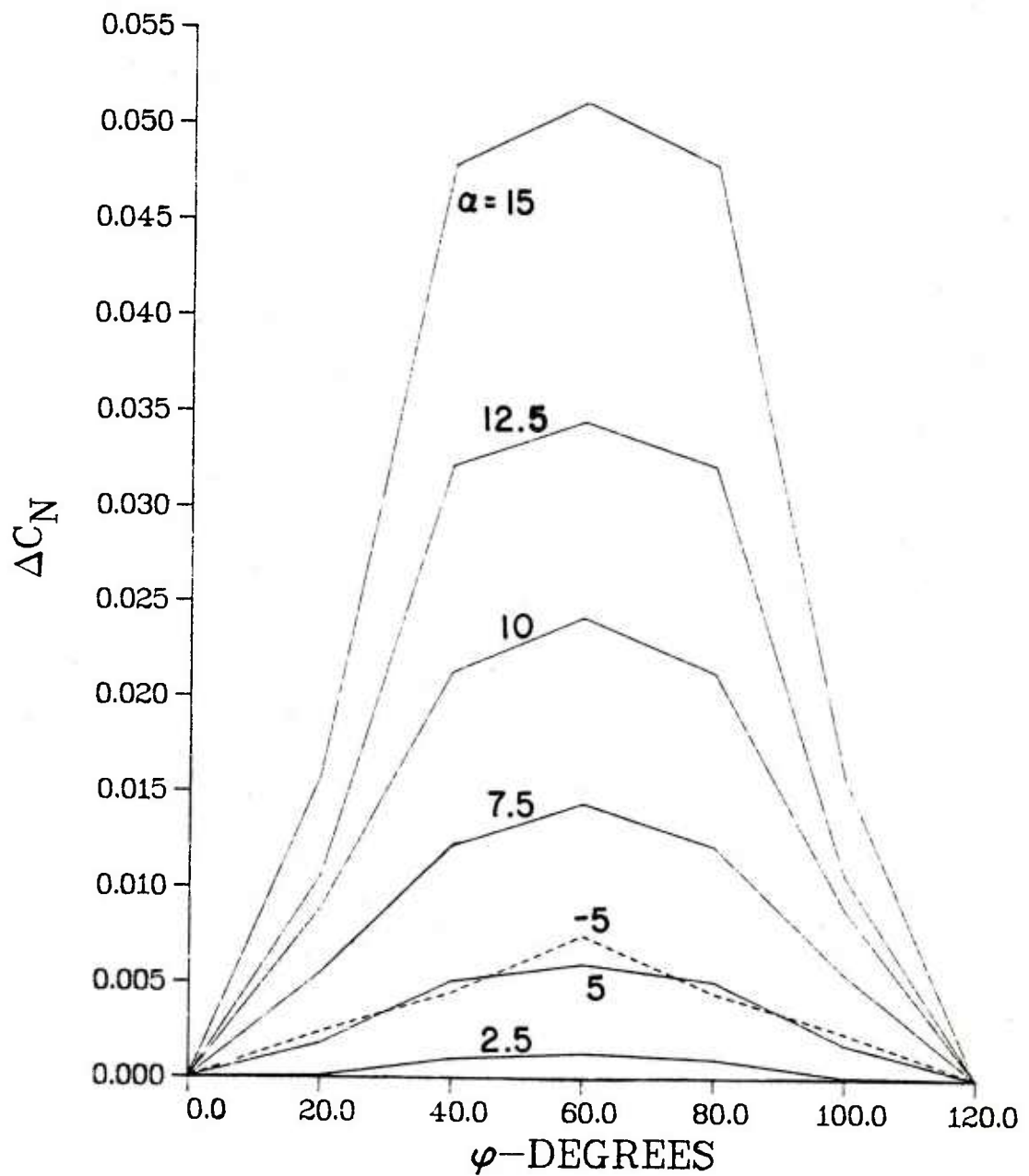


Figure 9. Incremental Coefficient Values, SOCBT-NC

a.  $\Delta C_N$  vs  $\phi$ ,  $M_\infty = 0.91$

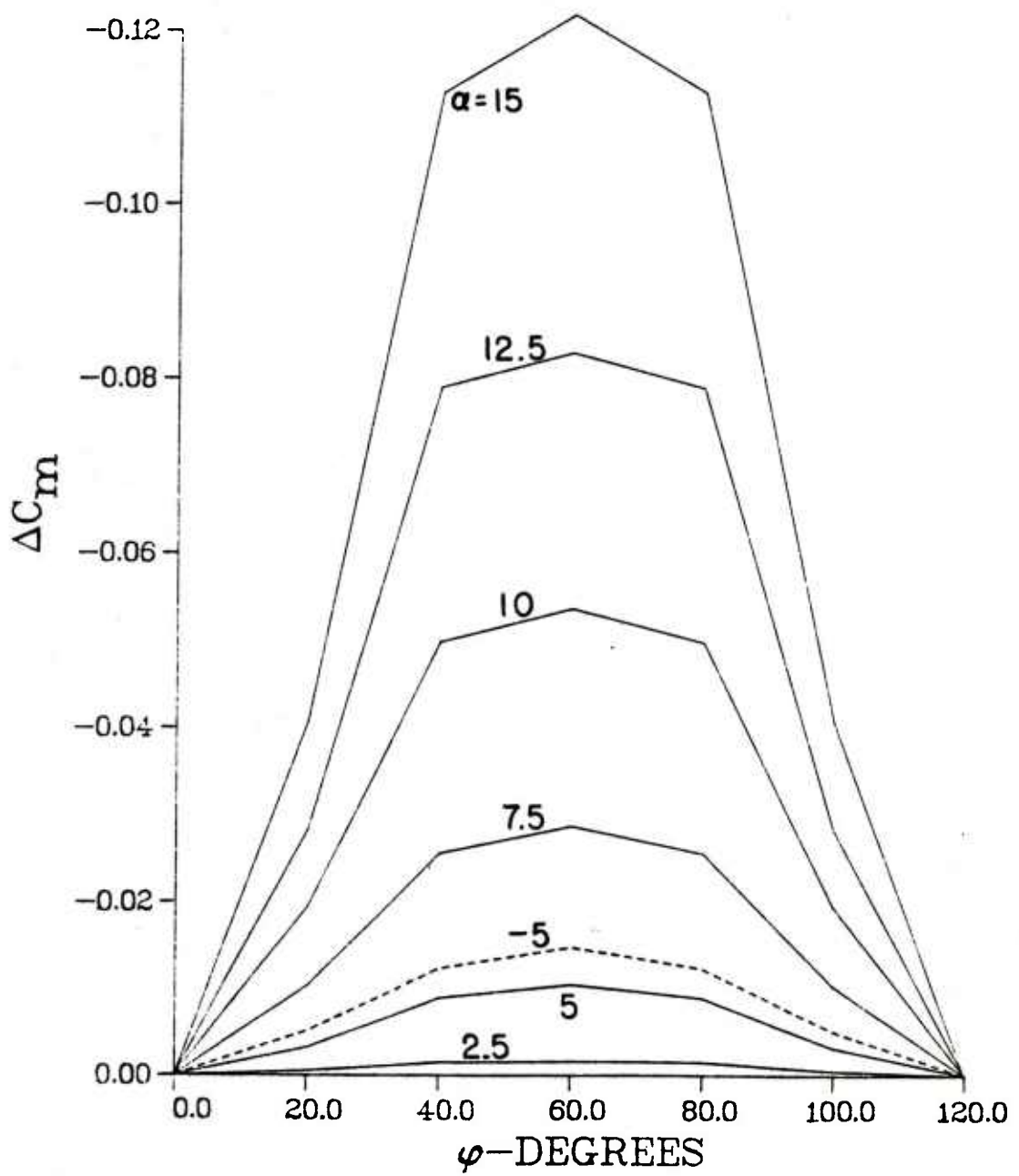


Figure 9. Continued

b.  $\Delta C_m$  vs  $\phi$ ,  $M_\infty = 0.91$

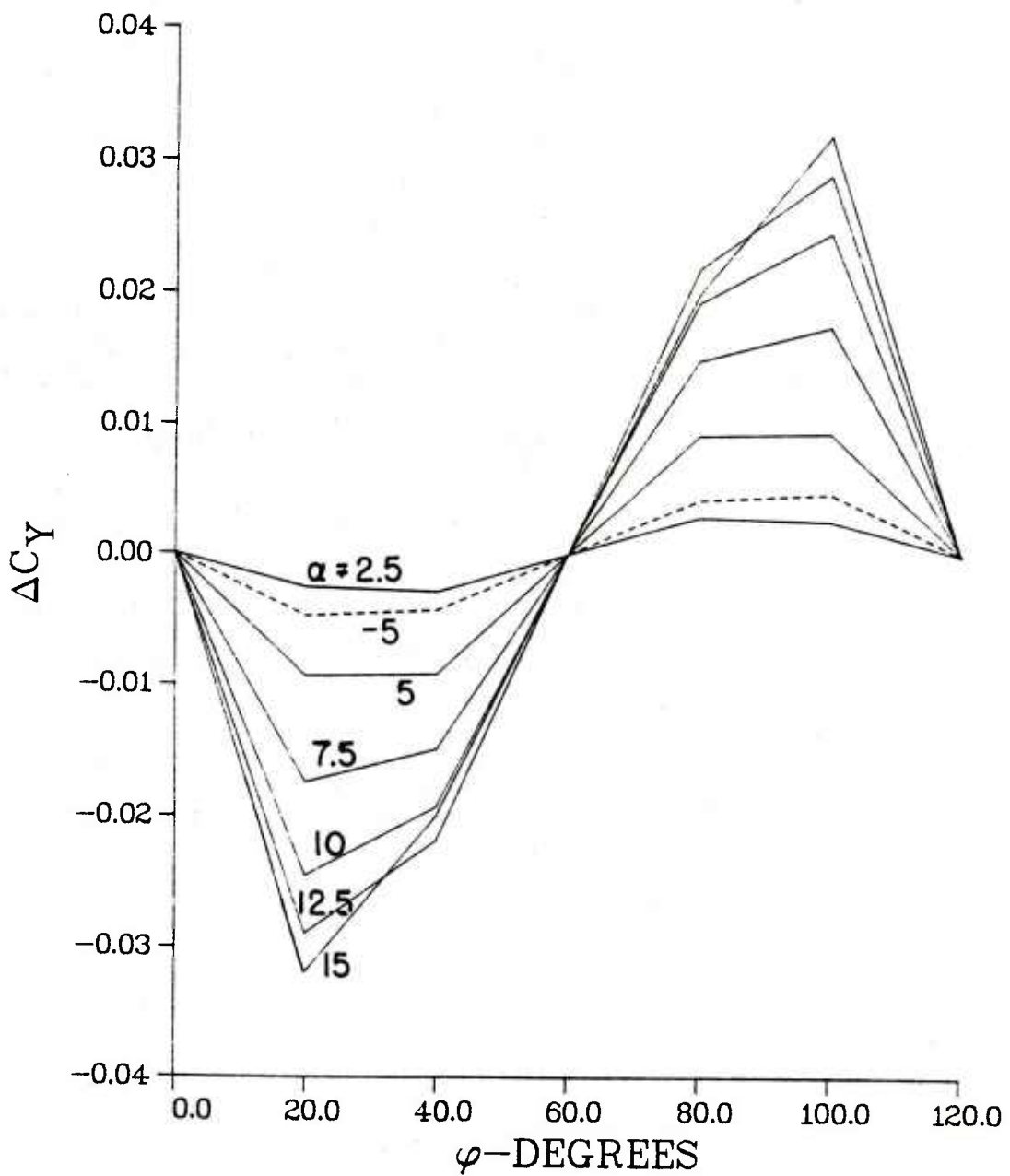


Figure 9. Continued

c.  $\Delta C_Y$  vs  $\phi$ ,  $M_\infty = 0.91$

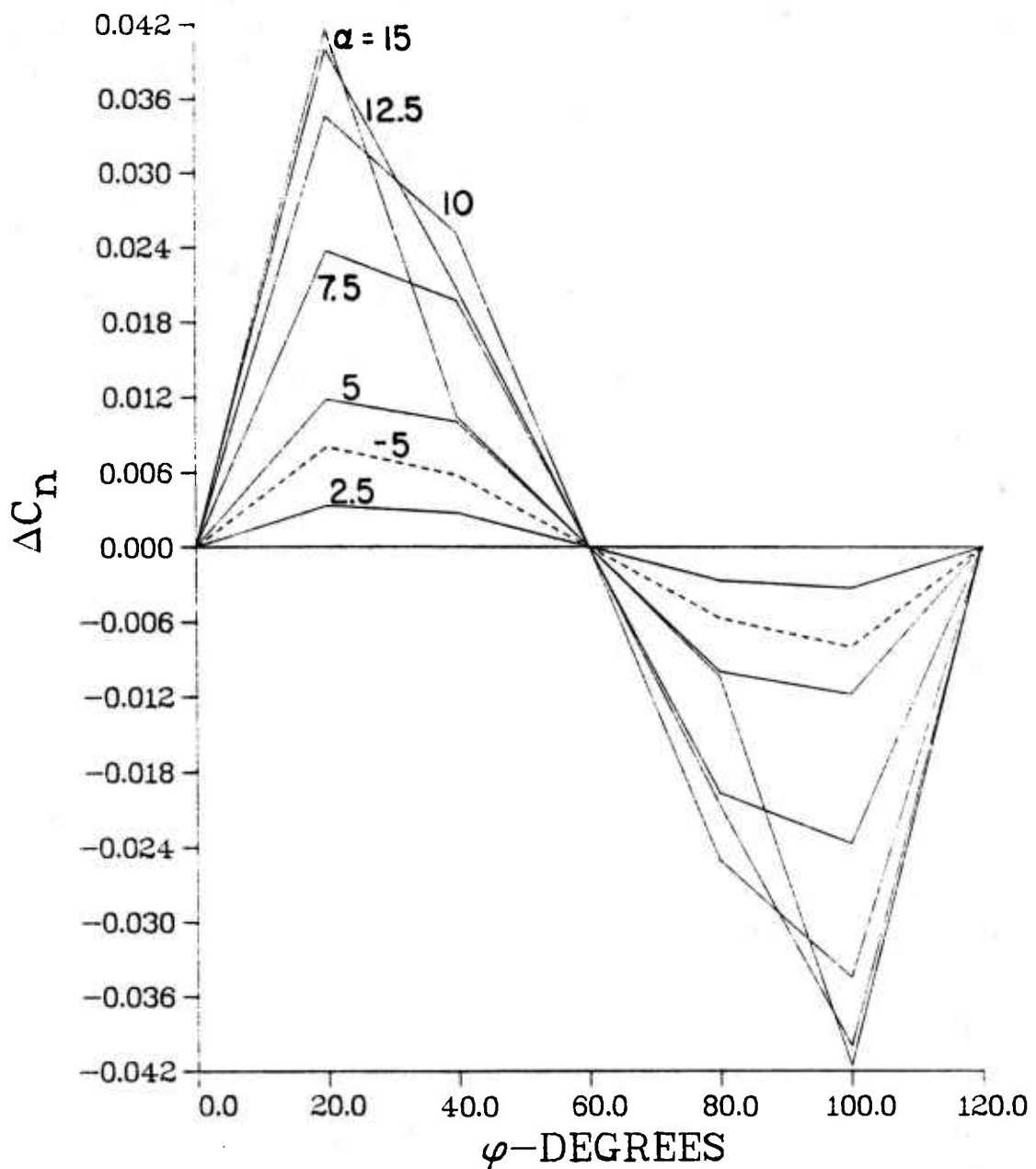


Figure 9. Continued

d.  $\Delta C_n$  vs  $\phi$ ,  $M_\infty = 0.91$

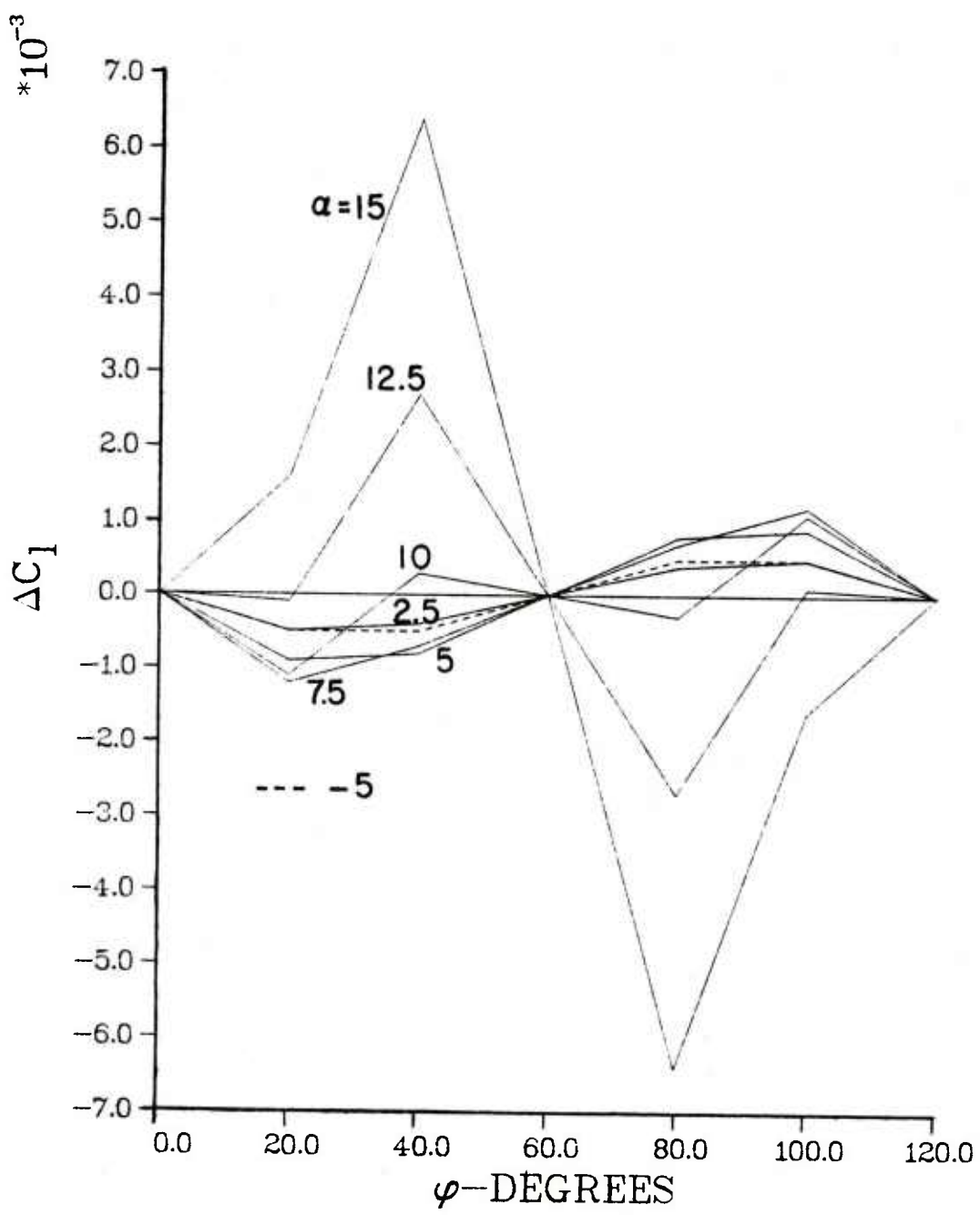


Figure 9. Continued

e.  $\Delta C_\lambda$  vs  $\phi$ ,  $M_\infty = 0.91$

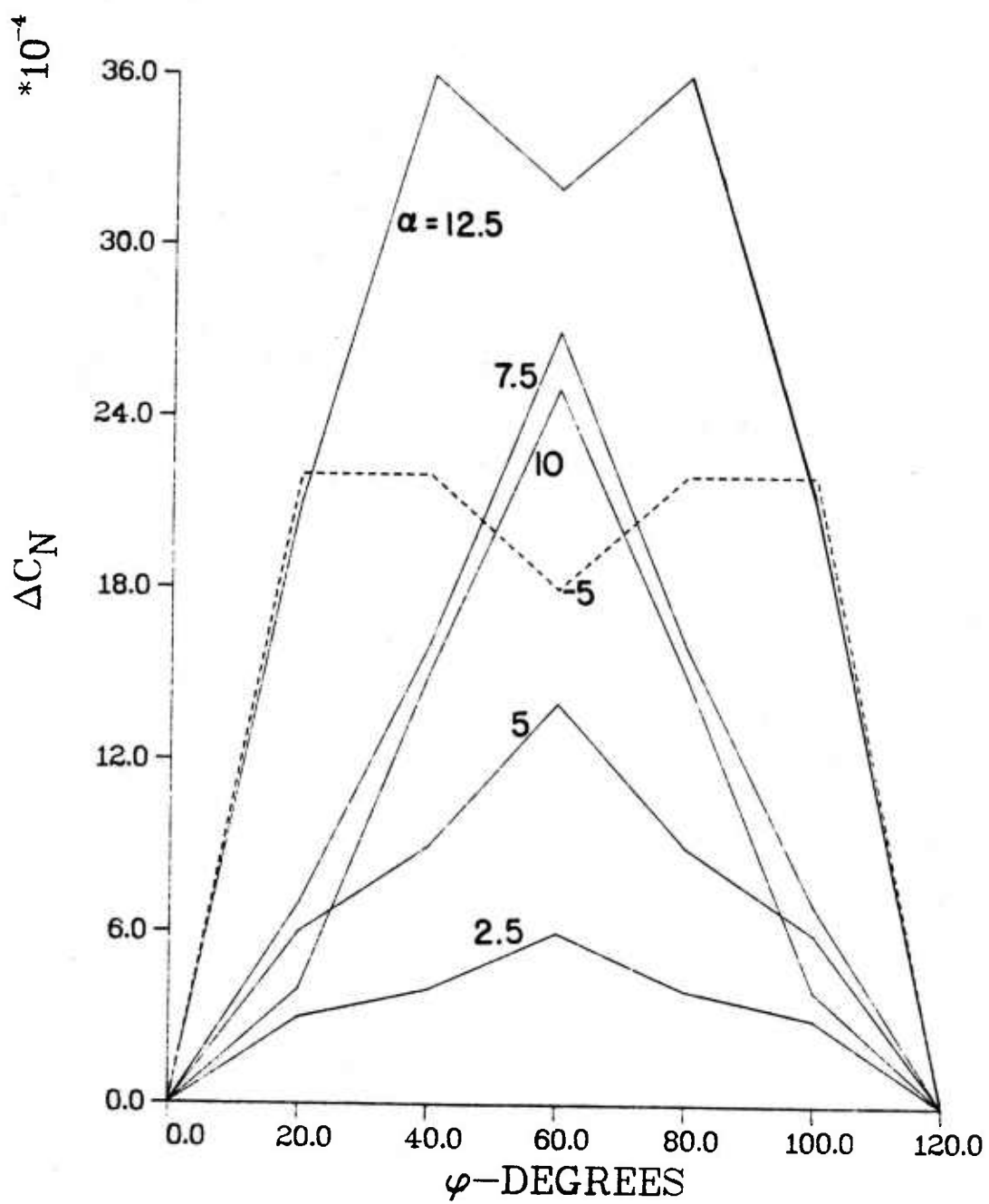


Figure 10. Incremental Coefficient Values, SOCBT-NC

a.  $\Delta C_N$  vs  $\phi$ ,  $M_\infty = 3.02$

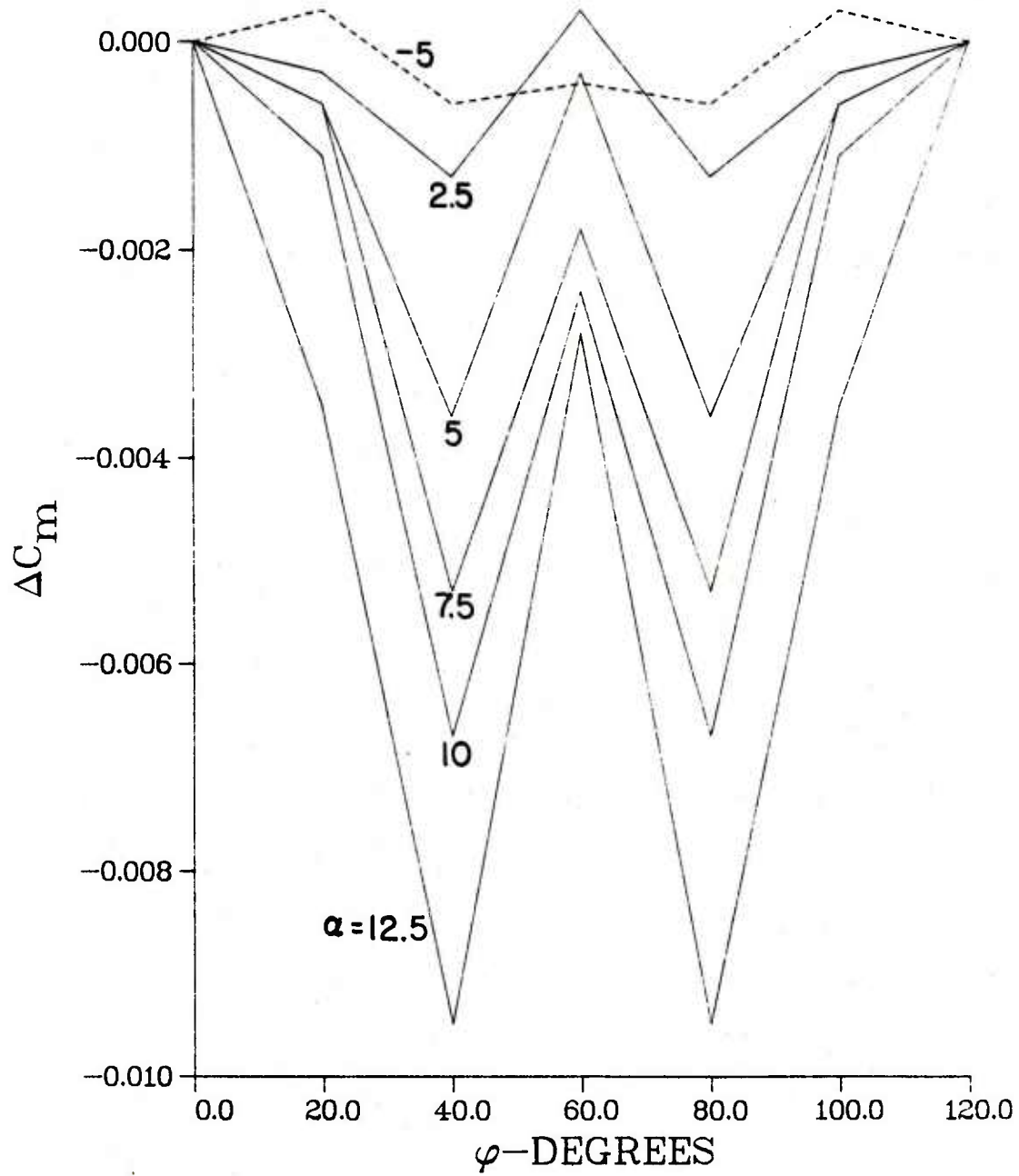


Figure 10. Continued

b.  $\Delta C_m$  vs  $\phi$ ,  $M_\infty = 3.02$

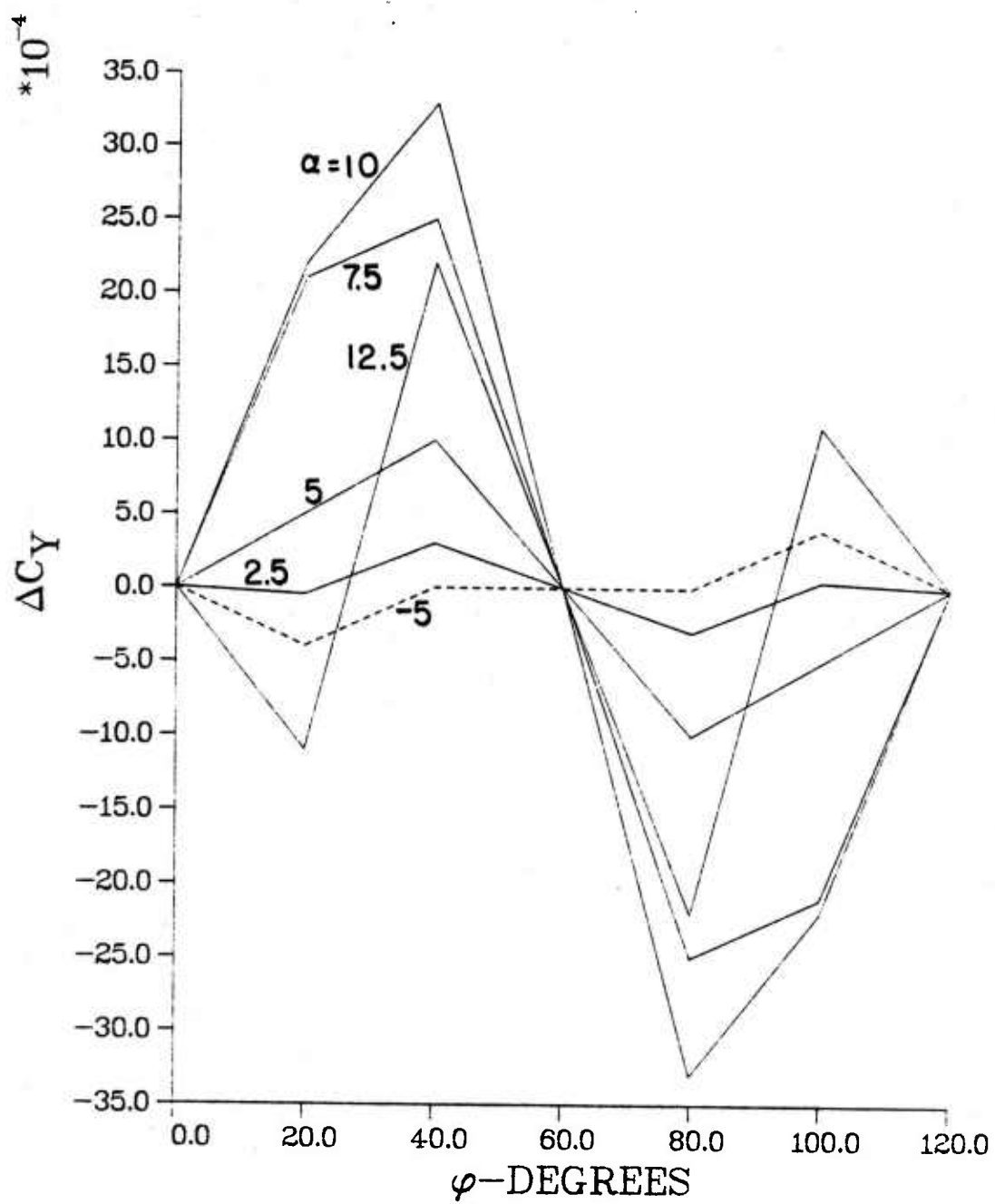


Figure 10. Continued

c.  $\Delta C_Y$  vs  $\phi$ ,  $M_\infty = 3.02$

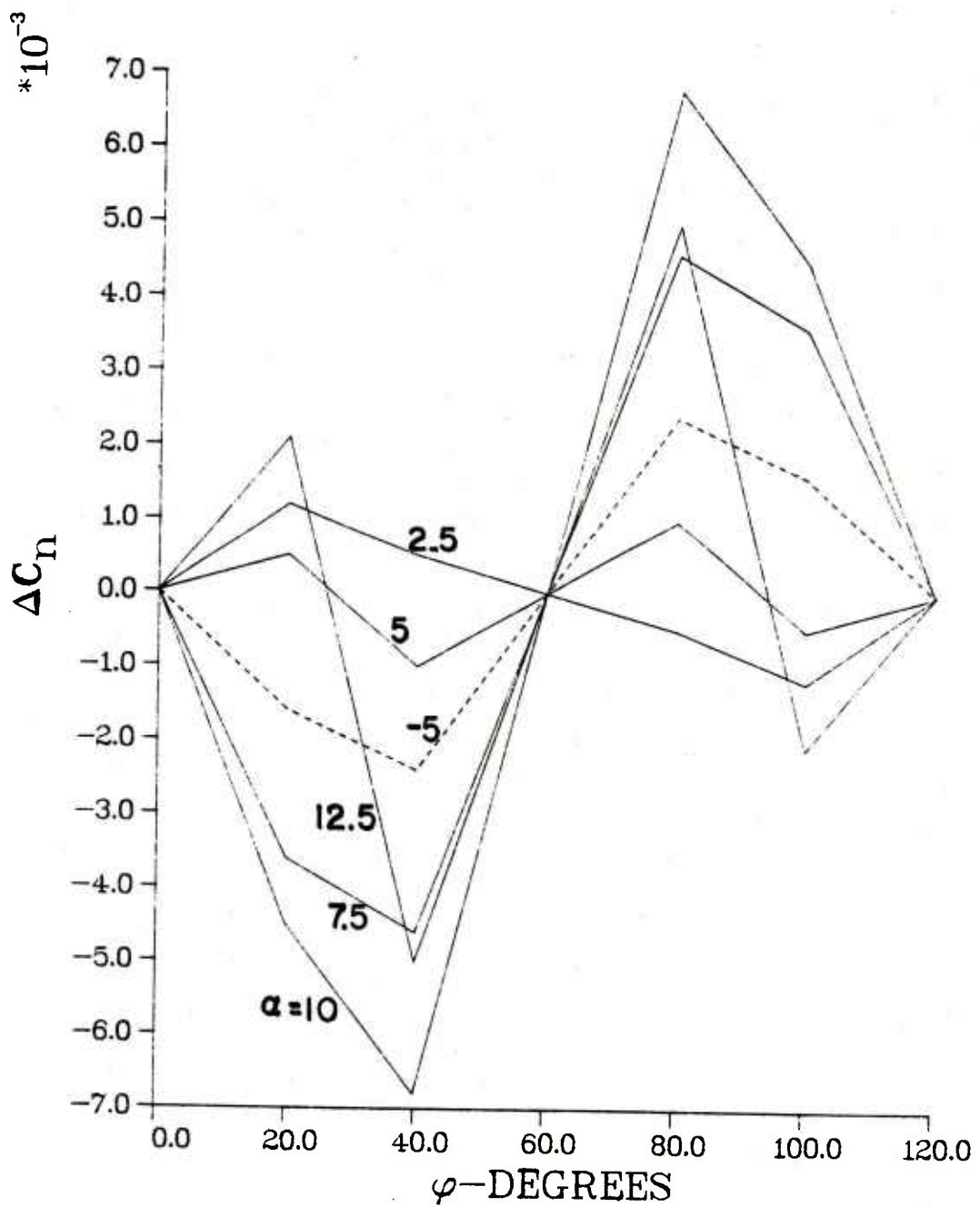


Figure 10. Continued

d.  $\Delta C_n$  vs  $\phi$ ,  $M_\infty = 3.02$

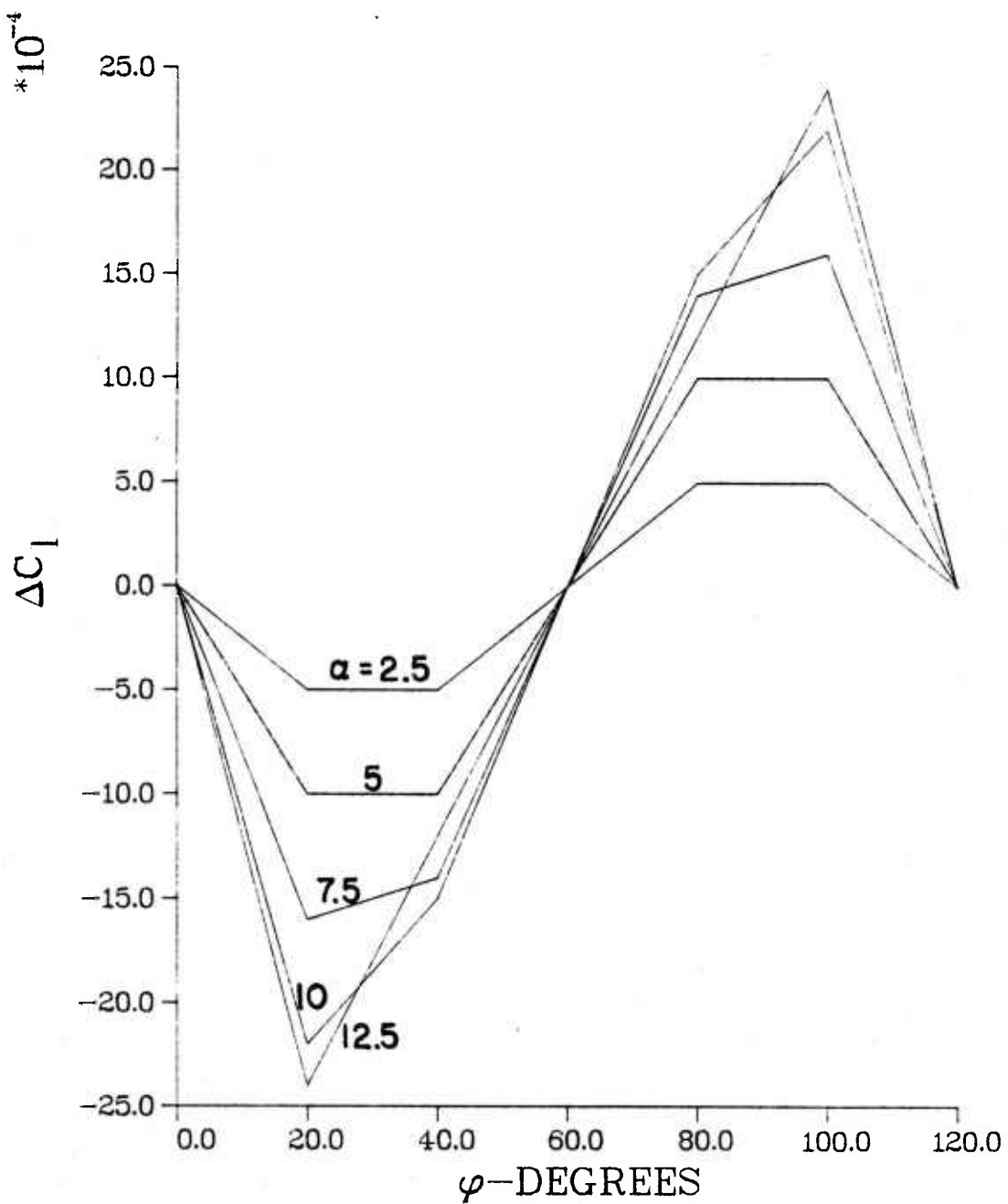


Figure 10. Continued

e.  $\Delta C_L$  vs  $\phi$ ,  $M_\infty = 3.02$

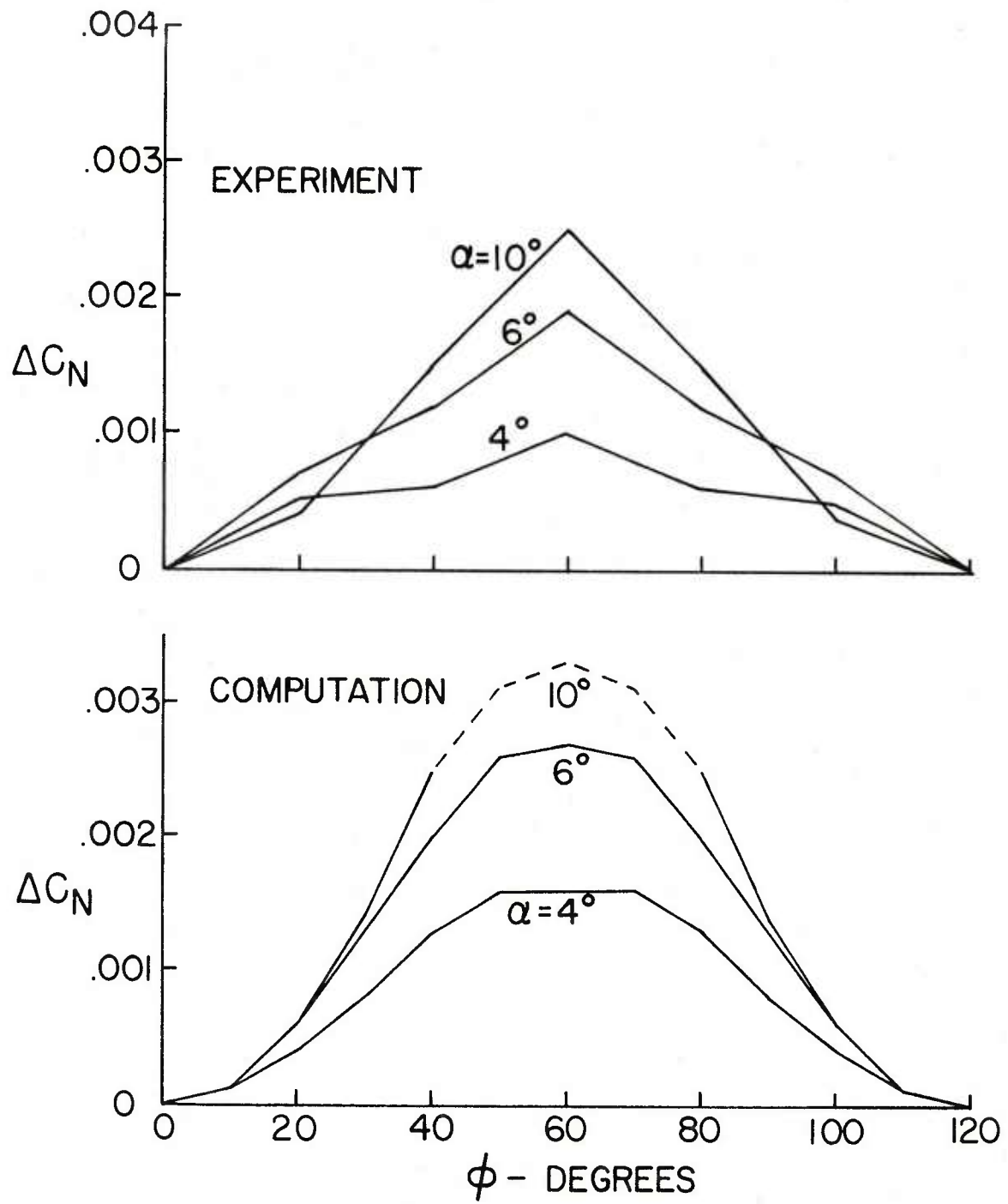


Figure 11. Incremental Normal Force Coefficients, Computation and Experiment,  $M_{\infty} = 3.02$

TABLE 1. ESTIMATED ERRORS

	<u>M = 0.91</u>		<u>M = 3.02</u>	
	<u>SD</u>	<u>1%*</u>	<u>SD</u>	<u>1%</u>
C <sub>N</sub>	0.2	2.0	0.1	2.1
Δ C <sub>N</sub>	3.1	29	27	500
C <sub>m</sub>	0.3	0.8	0.3	1.7
Δ C <sub>m</sub>	2.0	6.2	19.0	100
Δ C <sub>γ</sub>	35	23	18	400
Δ C <sub>n</sub>	29	9	40	70
Δ C <sub>λ</sub>	44	52	63	170

Errors - percent

$$SD = \frac{\text{Standard Deviation}}{\text{Max. Measurement}} \times 100$$

$$*1^\circ \text{ Criterion} = \frac{.01 \text{ (Full Scale)}}{\text{Max. Measurement}} \times 100$$

## REFERENCES

1. Platou, A.S., "An Improved Projectile Boattail," ARBRL-MR-2395, U.S. Army Ballistic Research Laboratory, ARRADCOM, Aberdeen Proving Ground, Maryland 21005, July 1974 (AD 785520).
2. Platou, A.S. and Nielson, G.I.T., "An Improved Projectile Boattail. Part II.," BRL R 1866, U.S. Army Ballistic Research Laboratory, ARRADCOM, Aberdeen Proving Ground, Maryland 21005, March 1976 (AD A024073).
3. Platou, A.S., "An Improved Projectile Boattail. Part III.," ARBRL-MR-2644, U.S. Army Ballistic Research Laboratory, ARRADCOM, Aberdeen Proving Ground, Maryland 21005, July 1976 (AD B012781L).
4. Platou, A.S., "An Improved Projectile Boattail. Part IV.," ARBRL-MR-02826, U.S. Army Ballistic Research Laboratory, ARRADCOM, Aberdeen Proving Ground, Maryland 21005, April 1978 (AD B027520L).
5. Zumwalt, G.W., "Experiments on Three-Dimensional Separating-and-Reattaching Flows," AIAA Paper No.81-0259, AIAA 19th Aerospace Sciences Meeting, January 1981.
6. Kayser, L.D. and Sturek, W.B., "Aerodynamic Performance of Projectiles With Axisymmetric and Non-Axisymmetric Boattails," ARBRL-MR-03022, U.S. Army Ballistic Research Laboratory, ARRADCOM, Aberdeen Proving Ground, Maryland 21005, May 1980 (AD A086091).
7. Schiff, L.B. and Sturek, W.B., "Numerical Simulation of Steady Supersonic Flow Over an Ogive Cylinder Boattail Body," ARBRL-TR-02363, U.S. Army Ballistic Research Laboratory, ARRADCOM, Aberdeen Proving Ground, Maryland 21005, September 1981 (AD A106060).
8. Danberg, J.E. and Tschirschnitz, R.H., "Transonic Pressure Distribution and Boundary Layer Characteristics of a Projectile With an Asymmetric Afterbody," Technical Report 243, University of Delaware, June 1981.
9. Platou, A.S., "Decreasing the Flight Time of Bullets by Improving Its Aerodynamic Characteristics," ARBRL-MR-03103, U.S. Army Ballistic Research Laboratory, ARRADCOM, Aberdeen Proving Ground, Maryland 21005, May 1981 (AD B058203L).
10. Schiff, L.B. and Steger, J.L., "Numerical Simulation of Steady Supersonic Flow," AIAA Journal, Vol. 18, No. 12, December 1980, pp. 1421-1430.

APPENDIX A. TABULATED DATA

## MACH=0.91      NORMAL FORCE COEFFICIENT

ALPHA	PPI=0	20	40	60	80	100	120
-5.0	-.1831	-.1802	-.1768	-.1749	-.1779	-.1786	-.1813
-2.5	-.0887	-.0872	-.0864	-.0869	-.0870	-.0886	-.0881
0.0	.0000	.0000	.0000	.0000	.0000	.0000	.0000
2.5	.0852	.0848	.0860	.0867	.0867	.0862	.0855
5.0	.1699	.1714	.1756	.1770	.1766	.1742	.1722
7.5	.2592	.2650	.2736	.2764	.2747	.2699	.2648
10.0	.3646	.3746	.3890	.3924	.3899	.3795	.3717
12.5	.4957	.5082	.5301	.5328	.5311	.5096	.5010
15.0	.6476	.6667	.6980	.7030	.7012	.6683	.6598

## MACH=0.91      PITCHING MOMENT COEFFICIENT

-5.0	-.3083	-.3124	-.3184	-.3234	-.3183	-.3100	-.3090
-2.5	-.1604	-.1607	-.1614	-.1633	-.1584	-.1504	-.1503
0.0	.0000	.0000	.0000	.0000	.0000	.0000	.0000
2.5	.1620	.1616	.1607	.1604	.1605	.1615	.1620
5.0	.3265	.3229	.3175	.3155	.3165	.3275	.3274
7.5	.4938	.4823	.4666	.4623	.4543	.4791	.4663
10.0	.6517	.6303	.5993	.5935	.5656	.6254	.6428
12.5	.7876	.7568	.7076	.7002	.7022	.7543	.7602
15.0	.9007	.8591	.7910	.7737	.7800	.8546	.8554

## MACH=0.91      DELTA NORMAL FORCE COEFFICIENT

-5.0	.0000	.0024	.0045	.0075	.0045	.0024	.0000
-2.5	.0000	-.0002	.0010	.0015	.0010	-.0002	.0000
0.0	.0000	.0000	.0000	.0000	.0000	.0000	.0000
2.5	.0000	.0001	.0010	.0013	.0010	.0001	.0000
5.0	.0000	.0018	.0051	.0060	.0051	.0018	.0000
7.5	.0000	.0055	.0122	.0144	.0122	.0055	.0000
10.0	.0000	.0089	.0213	.0242	.0213	.0089	.0000
12.5	.0000	.0106	.0322	.0345	.0322	.0106	.0000
15.0	.0000	.0158	.0479	.0512	.0479	.0158	.0000

## MACH=0.91      DELTA PITCHING MOMENT COEFFICIENT

-5.0	.0000	-.0051	-.0123	-.0148	-.0123	-.0051	.0000
-2.5	.0000	-.0010	-.0038	-.0034	-.0038	-.0010	.0000
0.0	.0000	.0000	.0000	.0000	.0000	.0000	.0000
2.5	.0000	-.0005	-.0015	-.0016	-.0015	-.0005	.0000
5.0	.0000	-.0032	-.0089	-.0105	-.0089	-.0032	.0000
7.5	.0000	-.0103	-.0256	-.0288	-.0256	-.0103	.0000
10.0	.0000	-.0194	-.0496	-.0537	-.0496	-.0194	.0000
12.5	.0000	-.0283	-.0790	-.0830	-.0790	-.0283	.0000
15.0	.0000	-.0407	-.1130	-.1219	-.1130	-.0407	.0000

## MACH=0.91      DELTA SIDE FORCE COEFFICIENT

ALPHA	PFI=0	20	40	60	80	100	120
-5.0	.0000	-.0048	-.0043	.0000	.0043	.0048	.0000
-2.5	.0000	-.0029	-.0026	.0000	.0026	.0029	.0000
0.0	.0000	.0000	.0000	.0000	.0000	.0000	.0000
2.5	.0000	-.0026	-.0029	.0000	.0029	.0026	.0000
5.0	.0000	-.0094	-.0092	.0000	.0092	.0094	.0000
7.5	.0000	-.0175	-.0149	.0000	.0149	.0175	.0000
10.0	.0000	-.0246	-.0193	.0000	.0193	.0246	.0000
12.5	.0000	-.0290	-.0219	.0000	.0219	.0290	.0000
15.0	.0000	-.0320	-.0200	.0000	.0200	.0320	.0000

## MACH=0.91      DELTA YAWING MOMENT COEFFICIENT

-5.0	.0000	.0080	.0057	.0000	-.0057	-.0080	.0000
-2.5	.0000	.0025	.0021	.0000	-.0021	-.0025	.0000
0.0	.0000	.0000	.0000	.0000	.0000	.0000	.0000
2.5	.0000	.0033	.0027	.0000	-.0027	-.0033	.0000
5.0	.0000	.0118	.0100	.0000	-.0100	-.0118	.0000
7.5	.0000	.0237	.0197	.0000	-.0197	-.0237	.0000
10.0	.0000	.0345	.0251	.0000	-.0251	-.0345	.0000
12.5	.0000	.0400	.0207	.0000	-.0207	-.0400	.0000
15.0	.0000	.0416	.0104	.0000	-.0104	-.0416	.0000

## MACH=0.91      DELTA ROLLING MOMENT COEFFICIENT

-5.0	.0000	-.0005	-.0005	.0000	.0005	.0005	.0000
-2.5	.0000	-.0004	-.0004	.0000	.0004	.0004	.0000
0.0	.0000	.0000	.0000	.0000	.0000	.0000	.0000
2.5	.0000	-.0005	-.0004	.0000	.0004	.0005	.0000
5.0	.0000	-.0009	-.0008	.0000	.0008	.0009	.0000
7.5	.0000	-.0012	-.0007	.0000	.0007	.0012	.0000
10.0	.0000	-.0011	-.0002	.0000	-.0003	.0011	.0000
12.5	.0000	-.0001	.0027	.0000	-.0027	.0001	.0000
15.0	.0000	.0016	.0064	.0000	-.0064	-.0016	.0000

## MACH=3.02      NORMAL FORCE COEFFICIENT

ALPHA	PHI=0	20	40	60	80	100	120
-5.0	-.2811	-.2819	-.2814	-.2806	-.2840	-.2636	-.2836
-2.5	-.1361	-.1364	-.1367	-.1371	-.1370	-.1368	-.1368
0.0	.0000	.0000	.0000	.0000	.0000	.0000	.0000
2.5	.1352	.1354	.1355	.1359	.1358	.1358	.1353
5.0	.2800	.2804	.2810	.2816	.2813	.2813	.2805
7.5	.4459	.4470	.4485	.4495	.4482	.4479	.4477
10.0	.6482	.6484	.6497	.6506	.6494	.6487	.6479
12.5	.8866	.8879	.8900	.8900	.8897	.8869	.8869

## MACH=3.02      PITCHING MOMENT COEFFICIENT

-5.0	-.2332	-.2328	-.2330	-.2340	-.2356	-.2339	-.2340
-2.5	-.1222	-.1224	-.1229	-.1228	-.1233	-.1224	-.1225
0.0	.0000	.0000	.0000	.0000	.0000	.0000	.0000
2.5	.1232	.1234	.1217	.1240	.1231	.1235	.1242
5.0	.2391	.2393	.2343	.2397	.2386	.2395	.2410
7.5	.3399	.3401	.3315	.3389	.3394	.3403	.3415
10.0	.4186	.4183	.4081	.4172	.4178	.4189	.4207
12.5	.4781	.4753	.4659	.4766	.4740	.4765	.4806

## MACH=3.02      DELTA NORMAL FORCE COEFFICIENT

-5.0	.0000	.0022	.0022	.0018	.0022	.0022	.0000
-2.5	.0000	-.0003	-.0005	-.0006	-.0005	-.0003	.0000
0.0	.0000	.0000	.0000	.0000	.0000	.0000	.0000
2.5	.0000	.0003	.0004	.0006	.0004	.0003	.0000
5.0	.0000	.0006	.0009	.0014	.0009	.0006	.0000
7.5	.0000	.0007	.0016	.0027	.0016	.0007	.0000
10.0	.0000	.0004	.0015	.0025	.0015	.0004	.0000
12.5	.0000	.0021	.0036	.0032	.0036	.0021	.0000

## MACH=3.02      DELTA PITCHING MOMENT COEFFICIENT

-5.0	.0000	.0003	-.0006	-.0004	-.0006	.0003	.0000
-2.5	.0000	.0003	-.0004	-.0004	-.0004	.0003	.0000
0.0	.0000	.0000	.0000	.0000	.0000	.0000	.0000
2.5	.0000	-.0003	-.0013	.0003	-.0013	-.0003	.0000
5.0	.0000	-.0006	-.0036	-.0003	-.0036	-.0006	.0000
7.5	.0000	-.0006	-.0053	-.0018	-.0053	-.0006	.0000
10.0	.0000	-.0011	-.0067	-.0024	-.0067	-.0011	.0000
12.5	.0000	-.0035	-.0095	-.0026	-.0095	-.0035	.0000

## MACH=3.02      DELTA SIDE FORCE COEFFICIENT

ALPHA	PHI=0	20	40	60	80	100	120
-5.0	.0000	-.0004	.0000	.0000	.0000	.0004	.0000
-2.5	.0000	-.0004	-.0004	.0000	.0004	.0004	.0000
0.0	.0000	.0000	.0000	.0000	.0000	.0000	.0000
2.5	.0000	.0000	.0003	.0000	-.0003	.0000	.0000
5.0	.0000	.0005	.0010	.0000	-.0010	-.0005	.0000
7.5	.0000	.0021	.0025	.0000	-.0025	-.0021	.0000
10.0	.0000	.0022	.0033	.0000	-.0033	-.0022	.0000
12.5	.0000	-.0011	.0022	.0000	-.0022	.0011	.0000

## MACH=3.02      DELTA YAWING MOMENT COEFFICIENT

-5.0	.0000	-.0016	-.0024	.0000	.0024	.0016	.0000
-2.5	.0000	-.0011	-.0006	.0000	.0006	.0011	.0000
0.0	.0000	.0000	.0000	.0000	.0000	.0000	.0000
2.5	.0000	.0012	.0005	.0000	-.0005	-.0012	.0000
5.0	.0000	.0005	-.0010	.0000	.0010	-.0005	.0000
7.5	.0000	-.0036	-.0046	.0000	.0046	.0036	.0000
10.0	.0000	-.0045	-.0068	.0000	.0068	.0045	.0000
12.5	.0000	.0021	-.0050	.0000	.0050	-.0021	.0000

## MACH=3.02      DELTA ROLLING MOMENT COEFFICIENT

-5.0	.0000	-.0010	-.0010	.0000	.0010	.0010	.0000
-2.5	.0000	-.0005	-.0005	.0000	.0005	.0005	.0000
0.0	.0000	.0000	.0000	.0000	.0000	.0000	.0000
2.5	.0000	-.0005	-.0005	.0000	.0005	.0005	.0000
5.0	.0000	-.0010	-.0010	.0000	.0010	.0010	.0000
7.5	.0000	-.0016	-.0014	.0000	.0014	.0016	.0000
10.0	.0000	-.0022	-.0015	.0000	.0015	.0022	.0000
12.5	.0000	-.0024	-.0012	.0000	.0012	.0024	.0000

## LIST OF SYMBOLS

$C_L$	rolling moment coefficient
$C_m$	pitching moment coefficient
$C_{m\alpha}$	slope of the pitching moment coefficient at $\alpha = 0$
$C_n$	yawing moment coefficient
$C_N$	normal force coefficient
$C_{N\alpha}$	slope of the normal force coefficient at $\alpha = 0$
$C_y$	side force coefficient
$M_\infty$	free-stream Mach number
SOC	figure 1 geometry with zero degree boattail angle
SOCBT	figure 1 geometry
SOCBT-NC	ogive-cylinder geometry of figure 1 with the boattail geometry of figure 2
$\alpha$	angle of attack, degrees
$\Delta C(\ )$	incremental coefficient values, for example, $\Delta C_N = C_N)_{\phi} - C_N)_{\phi = 0}; \phi \neq 0^\circ$
$\phi$	roll orientation of model, see figure 3

NOTE: The model diameter ( $d$ ), model cross section area ( $\pi d^2/4$ ), and the free-stream dynamic pressure were used to nondimensionalize forces and moments.

DISTRIBUTION LIST

<u>No. of Copies</u>	<u>Organization</u>	<u>No. of Copies</u>	<u>Organization</u>
12	Administrator Defense Technical Info Center ATTN: DTIC-DDA Cameron Station Alexandria, VA 22314	1	Director US Army Air Mobility Research and Development Laboratory Ames Research Center Moffett Field, CA 94035
1	Commander US Army Materiel Development and Readiness Command ATTN: DRCDMD-ST 5001 Eisenhower Avenue Alexandria, VA 22333	1	Commander US Army Communications Rsch and Development Command ATTN: DRSEL-ATDD Fort Monmouth, NJ 07703
9	Commander US Army Armament Research and Development Command ATTN: DRSMC-TDC DRSMC-TSS DRSMC-LCA-F Mr. D. Mertz Mr. E. Falkowski Mr. A. Loeb Mr. R. Kline Mr. S. Kahn Mr. H. Hudgins Dover, NJ 07801	1	Commander US Army Electronics Research and Development Command Technical Support Activity ATTN: DELSD-L Fort Monmouth, NJ 07703
1	Commander US Army Armament Materiel Readiness Command ATTN: DRSAR-LEP-L Rock Island, IL 61299	2	Commander US Army Missile Command ATTN: DRSMI-R DRSMI-RDK Mr. R. Deep Redstone Arsenal, AL 35898
1	Director US Army Armament Research and Development Command Benet Weapons Laboratory ATTN: DRDAR-LCB-TL Watervliet, NY 12189	1	Commander US Army Missile Command ATTN: DRSMI-YDL Redstone Arsenal, AL 35898
1	Commander US Army Aviation Research and Development Command ATTN: DRDAV-E 4300 Goodfellow Blvd. St. Louis, MO 63120	1	Commander US Army Tank Automotive Command ATTN: DRSTA-TSL Warren, MI 48090
1	Commander US Army Aviation Research and Development Command ATTN: DRDAV-E 4300 Goodfellow Blvd. St. Louis, MO 63120	1	Director US Army TRADOC Systems Analysis Activity ATTN: ATAA-SL White Sands Missile Range NM 88002
		1	Commander US Army Research Office P. O. Box 12211 Research Triangle Park NC 27709

## DISTRIBUTION LIST

<u>No. of Copies</u>	<u>Organization</u>	<u>No. of Copies</u>	<u>Organization</u>
1	Commander US Naval Air Systems Command ATTN: AIR-604 Washington, D. C. 20360	1	ACUREX Corporation/Aerotherm ATTN: Dr. M. J. Abbott 485 Clyde Avenue Mountain View, CA 94042
2	Commander David W. Taylor Naval Ship Research and Development Center ATTN: Dr. S. de los Santos Mr. Stanley Gottlieb Bethesda, Maryland 20084	1	Bendix Guided Systems Division ATTN: MS 2/17A (S. Wasserman) Teterboro, NJ 97608
4	Commander US Naval Surface Weapons Center ATTN: Dr. T. Clare, Code DK20 Mr. P. Daniels Mr. D. A. Jones III Mr. L. Mason Dahlgren, VA 22448	1	Nielsen Engineering & Research, Inc. ATTN: Dr. S. Stahara 510 Clyde Avenue Mountain View, CA 94043
4	Commander US Naval Surface Weapons Center ATTN: Code 312 Dr. W. Yanta Code R44 Dr. C. Hsieh Dr. T. Zien Dr. R. U. Jettmar Silver Spring, MD 20910	2	Sandia Laboratories ATTN: Technical Staff, Dr. W.L. Oberkampf Aeroballistics Division 5631, H.R. Vaughn Albuquerque, NM 87115
1	Commander US Naval Weapons Center ATTN: Code 3431, Tech Lib China Lake, CA 93555	1	Massachusetts Institute of Technology ATTN: Tech Library 77 Massachusetts Avenue Cambridge, MA 02139
1	Director NASA Langley Research Center ATTN: NS-185, Tech Lib Langley Station Hampton, VA 23365	1	University of Delaware Mechanical and Aerospace Engineering Department ATTN: Dr. J. E. Danberg Newark, DE 19711
2	Commandant US Army Infantry School ATTN: ATSH-CD-CSO-OR Fort Benning, GA 31905		<u>Aberdeen Proving Ground</u>
1	AFWL/SUL Kirtland AFB, NM 87117		Dir, USAMSAA ATTN: DRXSY-D DRXSY-MP, H. Cohen
			Cdr, USATECOM ATTN: DRSTE-TO-F
			Dir, USACSL, Bldg. E3516, EA ATTN: DRDAR-CLB-PA DRDAR-CLN DRDAR-CLJ-L

### USER EVALUATION OF REPORT

Please take a few minutes to answer the questions below; tear out this sheet, fold as indicated, staple or tape closed, and place in the mail. Your comments will provide us with information for improving future reports.

1. BRL Report Number \_\_\_\_\_

2. Does this report satisfy a need? (Comment on purpose, related project, or other area of interest for which report will be used.)  
\_\_\_\_\_  
\_\_\_\_\_  
\_\_\_\_\_

3. How, specifically, is the report being used? (Information source, design data or procedure, management procedure, source of ideas, etc.)  
\_\_\_\_\_  
\_\_\_\_\_  
\_\_\_\_\_

4. Has the information in this report led to any quantitative savings as far as man-hours/contract dollars saved, operating costs avoided, efficiencies achieved, etc.? If so, please elaborate.  
\_\_\_\_\_  
\_\_\_\_\_  
\_\_\_\_\_

5. General Comments (Indicate what you think should be changed to make this report and future reports of this type more responsive to your needs, more usable, improve readability, etc.)  
\_\_\_\_\_  
\_\_\_\_\_  
\_\_\_\_\_

6. If you would like to be contacted by the personnel who prepared this report to raise specific questions or discuss the topic, please fill in the following information.

Name: \_\_\_\_\_

Telephone Number: \_\_\_\_\_

Organization Address: \_\_\_\_\_  
\_\_\_\_\_  
\_\_\_\_\_